| | | | |
|---|---|---|---|
| | 0.020 | $5.77 \times 10^{2}$ | $1.73 \times 10^{-3}$ |
| | 0.030 | $7.59 \times 10^{2}$ | $1.32 \times 10^{-3}$ |
| 100 | 0.000 | $3.03 \times 10^{2}$ | $3.31 \times 10^{-3}$ |
| | 0.005 | $2.93 \times 10^{2}$ | $3.41 \times 10^{-3}$ |
| | 0.010 | $2.84 \times 10^{2}$ | $3.52 \times 10^{-3}$ |
| | 0.020 | $2.94 \times 10^{2}$ | $3.39 \times 10^{-3}$ |
| | 0.030 | $3.83 \times 10^{2}$ | $2.61 \times 10^{-3}$ |

**สมบัติเพียโซอิเล็กทริก**

สำหรับสมบัติเพียโซอิเล็กทริกนั้น ในการทดลองนี้ได้วัดค่าสัมประสิทธิ์เพียโซอิเล็กทริก ($d_{33}$) โดยการนำชิ้นงานเซรามิก $Bi_{0.5}Na_{0.5}Ti_{1-x}Co_xO_{3-x}$ ไปทำขั้วในน้ำมันซิลิโคน แต่เนื่องจากขาดเครื่องมือในการวัดวงฮีสเทอรีซีส จึงทำให้ไม่สามารถทราบค่าสนามไฟฟ้าลบล้าง ($E_c$) ทำให้ในการทำขั้วค่าสนามไฟฟ้าที่ใช้นำมาจากการอ้างอิงจากงานวิจัยอื่นๆ โดยได้ทดลองใช้สนามไฟฟ้ากระแสตรงเท่ากับ 3.5 kV/mm และ 4.5 kv/mm ซึ่งสามารถทำการทำขั้วได้โดยที่ชิ้นงานไม่เกิดการลัดวงจร โดยได้ทำการวัดค่าสัมประสิทธิ์เพียโซอิเล็กทริกของเซรามิกหลังการทำขั้วเสร็จทันทีและหลังการทำขั้วเป็นเวลา 24 ชั่วโมง

จากตาราง 4.36 และรูป 4.99 พบว่าเมื่อสนามไฟฟ้าที่ใช้ในการทำขั้วมีค่ามากขึ้นค่าสัมประสิทธิ์เพียโซอิเล็กทริกของเซรามิกมีค่าสูงขึ้น ทั้งนี้เนื่องมากจากค่าสนามไฟฟ้าที่มากขึ้นทำให้เกิดการจัดเรียงตัวของไดโพลโมเมนต์ตามสนามไฟฟ้ามากขึ้น เมื่อนำสนามไฟฟ้าออกโพลาไรเซชันคงค้างจึงมีมากขึ้นส่งผลให้เกิดการเหนี่ยวนำความต่างศักย์มากขึ้น เมื่อให้ความเค้นจากภายนอกแก่ชิ้นงานจึงทำค่าสัมประสิทธิ์เพียโซอิเล็กทริกมีค่าสูง เมื่อพิจารณาถึงเวลาที่ใช้ในการวัดพบว่า การทิ้งเซรามิกไว้เป็นเวลา 24 ชั่วโมงหลังการทำขั้วแล้วจึงทำการวัดให้ค่าสัมประสิทธิ์เพียโซอิเล็กทริกสูงกว่าการวัดทันทีหลังการทำขั้วเล็กน้อย ทั้งนี้อาจเนื่องมาจากการจัดเรียงตัวของไดโพลโมเมนต์บางส่วนที่ยังไม่สมบูรณ์หลังจากการเอาสนามไฟฟ้าออกเมื่อเวลาผ่านไป 24 ชั่วโมง ทำให้มีโพลาไรเซชันคงค้างสูงขึ้นอีกเล็กน้อย ค่าสัมประสิทธิ์เพียโซอิเล็กทริกจึงสูงขึ้น และเมื่อพิจารณาปริมาณการเจือ Co พบว่าค่าสัมประสิทธิ์เพียโซอิเล็กทริกมีแนวโน้มไปในทางเดียวกับค่าคงที่ไดอิเล็กทริก คือมีค่าสูงสุดและต่ำสุดที่ปริมาณ Co เท่ากับ 0.010 และ 0.030 เศษส่วนโดยโมล ตามลำดับ โดยค่าสัมประสิทธิ์เพียโซอิ

เล็กทริกสูงสุดที่ปริมาณ Co เท่ากับ 0.010 เศษส่วนโดยโมล อาจเนื่องมาจากเซรามิกมีความหนาแน่นสูงสุดและมีรูพรุนน้อย โดยค่าสัมประสิทธิ์เพียโซอิเล็กทริกสูงสุดมีค่าเท่ากับ 104.5 pC/N ที่การทำขั้วด้วยสนามไฟฟ้ากระแสตรง 4.5 kV/mm วัดหลังจากการทำขั้วเป็นเวลา 24 ชั่วโมง

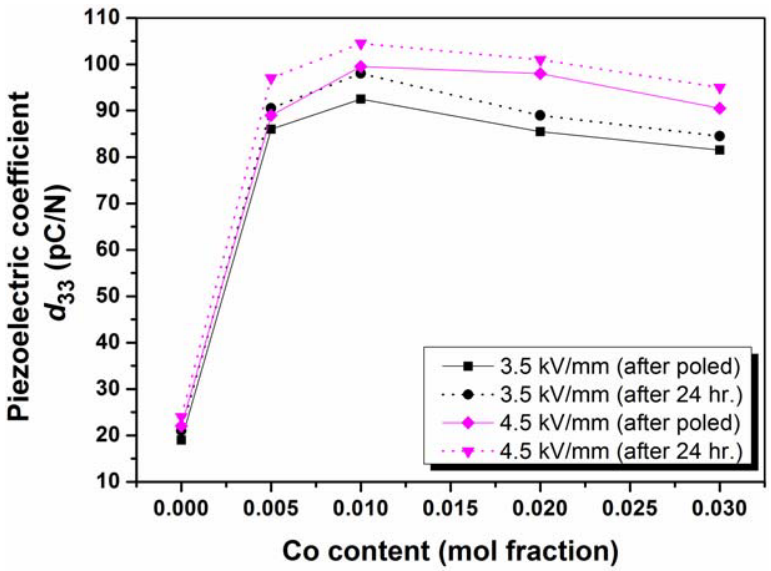


| Co content (mol fraction) | Piezoelectric coefficient ; $d_{33}$ (pC/N) (3.5 kV/mm DC field poled) | Piezoelectric coefficient ; $d_{33}$ (pC/N) (4.5 kV/mm DC field poled) |
|---|---|---|

รูป 4.99 กราฟค่าสัมประสิทธิ์เพียโซอิเล็กทริกของเซรามิก $Bi_{0.5}Na_{0.5}Ti_{1-x}Co_xO_{3-x}$ ที่ทำขั้วด้วยสนามไฟฟ้ากระแสตรง 3.5 kV/mm และ 4.5 kV/mm วัดหลังการทำขั้วทันทีและหลังทำขั้วเป็นเวลา 24 ชั่วโมง

| | after poled | after 24 hr. | after poled | after 24 hr. |
|---|---|---|---|---|
| 0.000 | 19.0 ± 1.41 | 21.0 ± 1.41 | 22.0 ± 1.41 | 24.0 ± 1.41 |
| 0.005 | 86.0 ± 0.00 | 90.5 ± 0.71 | 89.0 ± 0.00 | 97.0 ± 0.00 |
| 0.010 | 92.5 ± 0.71 | 98.0 ± 1.41 | 99.5 ± 3.54 | 104.5 ± 3.54 |
| 0.020 | 85.5 ± 0.71 | 89.0 ± 1.41 | 98.0 ± 4.24 | 101.0 ± 5.66 |
| 0.030 | 81.5 ± 0.71 | 84.5 ± 0.71 | 90.5 ± 0.71 | 95.0 ± 1.41 |

ตาราง 4.36 ค่าสัมประสิทธิ์เพียโซอิเล็กทริกของเซรามิก $Bi_{0.5}Na_{0.5}Ti_{1-x}Co_xO_{3-x}$ ที่ทำขั้วด้วยสนามไฟฟ้ากระแสตรง 3.5 kV/mm และ 4.5 kV/mm วัดหลังการทำขั้วทันที และหลังการทำขั้วเป็นเวลา 24 ชั่วโมง

# บทที่ 5
# สรุปผลการวิจัยและข้อเสนอแนะ

## 5.1 สรุปผลการวิจัย

การวิเคราะห์โครงสร้างผลึกของผง $Bi_{0.5}Na_{0.5}TiO_3$ โดยวิธีเรียทเวลด์อาศัยโปรแกรม General Structure Analysis System (GSAS) ซึ่งพบว่าจากคุณภาพของผงที่ใช้และข้อมูลของแผนภาพเลี้ยวเบนของรังสีเอกซ์ สามารถให้ค่า $R_p$ ของการเปรียบเทียบระหว่างแบบจำลองและข้อมูลจริงต่ำกว่า 5% ซึ่งแสดงให้เห็นว่า โครงสร้างผลึกที่ใช้รวมทั้งตัวแปรที่ปรับเปลี่ยนในโปรแกรมให้ผลโครงสร้างผลึกที่เชื่อถือได้ โดยพบว่าการวิเคราะห์โครงสร้างจากแผนภาพเลี้ยวเบนรังสีเอกซ์ให้โครงสร้างเป็นแบบรอมโบฮีดรอล

สำหรับผง $Bi_{0.5}Na_{0.5}Ti_{1-x}Zr_xO_3$ ได้ทำการวิเคราะห์ด้วยวิธีเลี้ยวเบนด้วยรังสีเอกซ์แล้ว พบว่า มีการขยับของพีคไปทางซ้ายทุกพีค ซึ่งแสดงให้เห็นถึงการขยายตัวของหน่วยเซลล์ นอกจากนี้ การเกิดการแยกตัวของพีคตรงตำแหน่งช่วง $2\theta$ = 45-50° และ 55-60° ในสารที่มี Zr เจือปนตั้งแต่ x = 0.55 ขึ้นไป แสดงให้เห็นว่าโครงสร้างผลึกมีการเปลี่ยนแปลง ยังมีความเป็นไปได้ที่จะมีเฟสอื่นปนอยู่ แต่การเจือปนของเฟสอื่นจะต้องมีการวิเคราะห์ด้านโครงสร้างจุลภาคเช่นกัน จากการตรวจสอบผลของอุณหภูมิที่ใช้ในการสังเคราะห์พบว่า อุณหภูมิ 800 °C ดูเหมือนจะเป็นอุณหภูมิที่ดีที่สุด เนื่องจากมีปริมาณของเฟสอื่นเจือปนต่ำมาก

การเตรียมผงของ $Bi_{0.5}Na_{0.5}ZrO_3$ พบว่าเงื่อนไขที่ดีที่สุดในการเตรียมผงเซรามิก BNZ ด้วยกระบวนการบดผสมออกไซด์ คือ BNZ/10wt%$Na_2CO_3$ โดยกระบวนการ double calcination ที่อุณหภูมิ 800 °C เป็นเวลา 2 ชั่วโมง เนื่องจากไม่มีเฟสของผงตั้งต้น $Bi_2O_3$ และ $ZrO_2$ ปรากฏอยู่ระหว่างมุม $2\theta$ = 25-30° เมื่อเปรียบเทียบกับผง BNZ ที่เตรียมด้วยสภาวะอื่นๆ ซึ่งเป็นกระบวนการที่ยังไม่มีนักวิจัยรายงานมาก่อน นอกจากนี้ การเตรียมเซรามิก BNZ ให้มีความหนาแน่นสูงนั้นยังต้องอาศัยปัจจัยอื่นเข้ามาช่วยด้วย เช่น การเติมสารช่วยเผา (sintering aid) เป็นต้น สภาวะการเตรียมผง BNZ ด้วยวิธีผสมออกไซด์ดีที่สุด คือ การเพิ่มปริมาณผงตั้งต้น $Na_2CO_3$ เท่ากับ 10 wt% และเผาแคลไซน์สองครั้งสารประกอบชนิดใหม่ BNZ เป็นวัสดุที่มีโครงสร้างแบบ perovskite และมีระบบผลึกเป็น orthorhombic โดยมี $Bi^{3+}$ และ $Na^{+}$ บรรจุตรงตำแหน่ง A และ $Zr^{4+}$ บรรจุตรงตำแหน่ง B ในโครงสร้าง

การเตรียมเซรามิก $Bi_{0.5}Na_{0.5}Ti_{0.41}Zr_{0.59}O_3$ เจือด้วยแลนทานัม พบว่าขนาดของเกรนเฉลี่ยมีค่าต่ำลงเมื่อปริมาณการเติมแลนทานัมสูงขึ้น นอกจากนี้ สมบัติไดอิเล็กทริกของเซรามิกนี้มีแนวโน้มที่ดีขึ้นเมื่อเจือแลนทานัมเพิ่มขึ้น ซึ่งเป็นไปตามลักษณะของการเจือวัสดุเพียโซอิเล็กทริกด้วยไอออนที่มีประจุสูงกว่าไอออนในสารหลัก โดยจะส่งผลให้การเคลื่อนที่ของโดเมนไฟฟ้าดีขึ้น อย่างไรก็ตาม สมบัติทางเฟร์โรอิเล็กทริกมีค่าไม่ดีนัก อาจจะเนื่องมาจากวัสดุนี้ มีการสูญเสียเนื่องจากการนำไฟฟ้าที่ค่อนข้างสูงทำให้ค่าโพลาไรเซชันคงเหลือมีค่าต่ำเมื่อเทียบกับสารเพียโซอิเล็กทริกชนิดอื่น

การเตรียมเซรามิก $Bi_{0.5}Na_{0.5}Ti_{0.41}Zr_{0.59}O_3$ เจือด้วยไนโอเบียม พบว่าขนาดของเกรนมีแนวโน้มลดลงเช่นกัน ซึ่งดูเหมือนว่าจะเป็นแนวโน้มปกติของสารที่เจือด้วยตัวให้ (donor) จากการวัดสภาพต้านทานไฟฟ้าที่อุณหภูมิห้องพบว่า มีแนวโน้มที่ต่ำลงเมื่อปริมาณไนโอเบียมสูงขึ้น ซึ่งแสดงให้เห็นถึงว่าวัสดุมีการนำไฟฟ้าที่ดีขึ้น ส่วนค่าคงที่ไดอิเล็กทริกพบว่ามีค่าสูงสุดเมื่อเติมไนโอเบียมในปริมาณ 0.05 เศษส่วนโดยโมล

จากการศึกษาสาร $Bi_{0.5}Na_{0.5}Ti_{1-x}Co_xO_{3-x}$ ที่ปริมาณการเจือ Co เท่ากับ 0.000, 0.005, 0.010, 0.020, 0.030 มีโครงสร้างผลึกยังคงเป็นแบบรอมโบฮีดรอลเช่นเดียวกับ BNT บริสุทธิ์ และไม่พบเฟสแปลกปลอมเกิดขึ้น ในส่วนของเซรามิก การเจือ Co ไม่ทำให้เกิดการเปลี่ยนแปลงเฟส และการเคลื่อนตัวของพีคมีแนวโน้มไม่ชัดเจน แต่ปรากฏพีคที่มีลักษณะที่แตกต่างกันตามปริมาณ ความหนาแน่นของเซรามิกมีแนวโน้มเพิ่มขึ้นในระดับหนึ่ง และลดลงเมื่อเพิ่มปริมาณ Co สูงขึ้น โดยที่ Co 0.010 เศษส่วนโดยโมล มีค่าความหนาแน่นสูงสุด โครงสร้างทางจุลภาคมีเกรนรูปร่างแบบอิควิแอกซ์ และมีขนาด

เกรนใหญ่ขึ้นตามปริมาณการเจือ Co การศึกษาสมบัติเชิงกล พบว่าค่าความแข็งแบบวิกเกอร์สมีแนวโน้มเช่นเดียวกับค่าความหนาแน่น โดยมีค่าสูงสุดที่ปริมาณการเจือ Co 0.010 เศษส่วนโดยโมล การศึกษาสมบัติทางไฟฟ้าของเซรามิก พบว่าค่าคงที่ไดอิเล็กทริก ค่าสัมประสิทธิ์การนำไฟฟ้า และสัมประสิทธิ์เพียโซอิเล็กทริก มีแนวโน้มเพิ่มขึ้นในช่วงแรกโดยมีค่าสูงสุดที่ปริมาณการเจือ Co เท่ากับ 0.010 เศษส่วนโดยโมล และมีแนวโน้มลดลงเมื่อปริมาณ Co เพิ่มขึ้น

## 5.2 **ข้อเสนอแนะ**

สำหรับผลของการวิเคราะห์โครงสร้างผลึกโดยวิธีเรียทเวลด์ สามารถนำไปขยายไปสู่การศึกษาในเชิงทฤษฎี เช่น เมื่อทราบตำแหน่งของอะตอมสามารถนำไปหาโครงสร้างทางอิเล็กทรอนิกส์ของสารประกอบออกไซด์ที่สนใจได้ หรือเมื่อทราบถึงขนาดของการสั่นของอะตอม สามารถนำไปประมาณหาสภาพนำความร้อนของวัสดุได้ เป็นต้น โดยข้อมูลดังกล่าว สามารถถูกใช้ไปประเมินสมบัติทางเทอร์โมอิเล็กทริกของวัสดุ ซึ่งจะเป็นประโยชน์ต่องานวิจัยและการพัฒนาอุปกรณ์ที่จะนำมาประยุกต์ด้านพลังงานทดแทนต่อไปในอนาคต

# เอกสารอ้างอิง


[1] H.M. Rietveld, Line profiles of netron powder-diffraction peaks for structure refinement, *Acta Crystallographica* 22 (1967) 151-152.

[2] H.M. Rietveld, A profile refinement method for nuclear and mangnetic structure, *Journal of Appied. Crystallography* 2 (1969) 65-71.

[3] G.L. Lager, T. Armbruster and J. Faber, Neutron and X-ray diffraction study of hydrogarnet $Ca_3Al_2(O_4H_4)_3$, *American Mineral* 69 (1987) 756-765.

[4] A. Williams, G.H. Kwei, R.B. Von Dreele, A.C. Larson, I.D. Raistrick and D.L. Bish, Joint X-ray and neutron refinement of the structure of superconducting $YBa_2Cu_3O_{7-x}$: Precision structure, anisotropic thermal parameters, strain, and cation disorder. *Physical Review B37* (1988) 7960-7962.

[5] R.A. Young, *The Rietveld Method*, edited by R.A. Young, Ch.1, Oxford University Press (1993), pp. 1-38.

[6] A.C. Larson and R.B. Von Dreele, "General Structure Analysis System (GSAS)", Los Alamos National Laboratory Report LAUR 86-748 (2000).

[7] B.H. Toby, EXPGUI, a graphical user interface for GSAS, *Journal of Applied Crystallography* 34 (2001) 210-213.

[8] S. Bid, P. Sahu and S.K. Pradhan, Microstructure characterization of mechanosynthesized nanocrystalline $NiFe_2O_4$ by Rietveld's analysis, *Physica E: Low-dimensional Systems and Nanostructures* 39, 2 (2007) 175-184.

[9] P. Pourghahramani and E. Forssberg, The characterization of structural changes in hematite ground in a confined particle bed using Rietveld analysis, *International Journal of Mineral Processing*, Volume 83, Issues 1-2, 4 July 2007, Pages 47-59.

[10] H. Dutta, M. Sinha, Y.C. Lee and S.K. Pradhan, Microstructure characterization and phase transformation kinetics of ball-mill prepared nanocrystalline Mg–Zn-ferrite by Rietveld's analysis and electron microscopy, *Materials Chemistry and Physics* 105, 1, (2007) 31-37.

[11] M. Mir, C.C de Paula, D. Garcia, R.H.G.A. Kiminami, J.A. Eiras and Y.P. Mascarenhas, Microstructural characterization using the Rietveld method in lead lanthanum titanate ceramics system produced by combustion synthesis, *Journal of the European Ceramic Society* 27, 13-15 (2007) 3719-3721.

[12] H. Wei, Z. Jiliang and Z. Lingmin, Rietveld Refinement of New Ternary Compound $Al_{14}Dy_5Si$, *Journal of Rare Earths* 24, 1, Suppl.1 (2006) 78-81.

[13] J.R. Martínez, S. Palomares-Sánchez, G. Ortega-Zarzosa, Facundo Ruiz and Yurii Chumakov, Rietveld refinement of amorphous $SiO_2$ prepared via sol–gel method, *Materials Letters* 60, 29-30 (2006) 3526-3529.

[14] F. Guirado and S. Gali Quantitative Rietveld analysis of CAC clinker phases using synchrotron radiation, *Cement and Concrete Research* 36, 11 (2006) 2021-2032.

[15] M. Karolus and E. Lagiewka, Structure studies of $Fe_{81}Nb_5B_{14}$ annealed alloys by Rietveld refinement, J*ournal of Alloys and Compounds* 423, 1-2, 26 (2006) 92-95.

[16] R.M. Wilson, S.E.P. Dowker and J.C. Elliott, Rietveld refinements and spectroscopic structural studies of a Na-free carbonate apatite made by hydrolysis of monetite, *Biomaterials* 27, 27 (2006) 4682-4692.

[17] P. Jha and A.K. Ganguli, New perovskite oxides of the type $(Ln_{1/3}Ba_{1/3}Ca_{1/3})(Zn_{1/3}Ti_{2/3})O_{3-\delta}$: Rietveld analysis and dielectric properties, *Materials Chemistry and Physics* 97, 2-3 (2006) 337-342.

[18] W. Paszkowicz and J.A. Leiro, Rietveld refinement study of pyrite crystals, *Journal of Alloys and Compounds* 401, 1-2 (2005) 289-295.

[19] T. Yao, N. Ozawa, T. Aikawa and S. Yoshinaga, Analysis of layered structures of lithium–graphite intercalation compounds by one-dimensional Rietveld method, *Solid State Ionics* 175, 1-4 (2004) 199-202.

[20] D. Dermatas and M. S. Dadachov, Rietveld quantification of montmorillonites in lead-contaminated soils, *Applied Clay Science* 23, 1-4 (2003) 245-255.

[21] P. Bonneau, P. Garnier, G. Calvarin, E. Husson, J. R. Gavarri, A. W. Hewat and A. Morell, X-ray and neutron diffraction studies of the diffuse phase transition in $PbMg_{1/3}Nb_{2/3}O_3$ ceramics, *Journal of Solid State Chemistry* 91, 2 (1991) 350-361.

[22] H. Liu and H. Toraya, Study on a new tetragonal phase of Nb-doped lead titanate zirconate by synchrotron X-ray powder diffraction, *Journal of Physics and Chemistry of Solids* 60, 6 (1999) 729-735.

[23] C. Bedoya, Ch. Muller, J. -L. Baudour, V. Madigou, M. Anne and M. Roubin, Sr-doped $PbZr_{1-x}Ti_xO_3$ ceramic: structural study and field-induced reorientation of ferroelectric domains, *Materials Science and Engineering B* 75, 1 (2000) 43-52.

[24] W. Dmowski, M. K. Akbas, T. Egami and P. K. Davies, Structure refinement of large domain relaxors in the $Pb(Mg_{1/3}Ta_{2/3})O_3$–$PbZrO_3$ system, *Journal of Physics and Chemistry of Solids* 63, 1 (2002) 15-22.

[25] R. Bertram, G. Reck and R. Uecker, Growth and correlation between composition and structure of $(1-x)Pb(Zn_{1/3}Nb_{2/3})O_3$-$xPbTiO_3$ crystals near the morphotropic phase boundary, *Journal of Crystal Growth* 253, 1-4 (2003) 212-220.

[26] J. C. Bruno, A. A. Cavalheiro, M. A. Zaghete, M. Cilense and J. A. Varela, Structural effects of Li and K additives on the columbite precursor and 0.9PMN–0.1PT powders, *Materials Chemistry and Physics* 84, 1 (2004) 120-125.

[27] M. Mir, C.C de Paula, D. Garcia, R.H.G.A. Kiminami, J.A. Eiras and Y.P. Mascarenhas, Microstructural characterization using the Rietveld method in lead lanthanum titanate ceramics system produced by combustion synthesis, *Journal of the European Ceramic Society* 27, 13-15 (2007) 3719-3721.

[28] J.R.R. Siqueira, A.Z. Simões, B.D. Stojanovic, C.O. Paiva-Santos, L.P.S. Santos, E. Longo and J.A. Varela, Influence of milling time on mechanically assisted synthesis of $Pb_{0.91}Ca_{0.1}TiO_3$ powders, *Ceramics International* 33, 6 (2007) 937-941.

[29] A. Sani, M. Hanfland and D. Levy, Pressure and temperature dependence of the ferroelectric-paraelectric phase transition in $PbTiO_3$, *Journal of Solid State Chemistry* 167 (2002) 446-452.

[30] S. Suasmoro, S. Pratapa, D. Hartanto, D. Setyoko and U. M. Dani, The characterization of mixed titanate $Ba_{1-x}Sr_xTiO_3$ phase formation from oxalate coprecipitated precursor, *Journal of the European Ceramic Society* 20, 3 (2000) 309-314.

[31] A. Feteira, G. M. Keith, M. J. Rampling, C. A. Kirk, I. M. Reaney, K. Sarma, N. Mc. Alford and D. C. Sinclair, Synthesis and characterisation of Ga-doped hexagonal $BaTiO_3$, *Crystal Engineering* 5, 3-4 (2002) 439-448.

[32] S. Khemakhem, S. Yahyaoui, R. B. Hassen, H. Khemakhem and A. B. Salah, Crystal structure and electrical behavior of the new ceramic $Ba_{0.7}Na_{0.3}Ti_{0.7}Nb_{0.3}O_3$, *Solid State Sciences* 5, 2 (2003) 367-371.

[33] J.R. Sambrano, E. Orhan, M.F.C. Gurgel, A.B. Campos, M.S. Góes, C.O. Paiva-Santos, J.A. Varela and E. Longo, Theoretical analysis of the structural deformation in Mn-doped $BaTiO_3$, *Chemical Physics Letters* 402, 4-6 (2005) 491-496.

[34] K. Suzuki and K. Kijima, Phase transformation of $BaTiO_3$ nanoparticles synthesized by RF-plasma CVD, *Journal of Alloys and Compounds* 419, 1-2 ( 2006) 234-242.

[35] S. Anwar, P.R. Sagdeo, N.P. Lalla, Locating the normal to relaxor phase boundary in $Ba(Ti_{1-x}Hf_x)O_3$ ceramics, *Materials Research Bulletin* (2007) (in press).

[36] C.F. Buhrer, *Journal of Chemistry and Physics* 36 (1962) 798.

[37] K. Roleder, J. Suchanicz and A. Kania, *Ferroelectrics* 89 (1989) 1.

[38] A. Sasaki, T. Chiba, Y. Mamiya and E. Otsuki, *Japanese Journal of Applied Physics* 38 (1999) 5564.

[39] T. Takenaka, K.-I. Maruyama and K. Sakata, *Japanese Journal of Applied Physics* 30, 9B (1991) 2236.

[40] G.O. Jones and P.A. Thomas, Investigation of the structure and phase transitions in the novel A-site substituted distorted perovskite compound $Na_{0.5}Bi_{0.5}TiO_3$, *Acta Crystallographica* B58 (2002) 168-178.

[41] Nolze G., and Kraus W., *Powder Cell – a program for the representation and manipulation of crystal structures and calculation of the resulting X-ray powder patterns.* Journal of Applied Crystallography, 1996; 29: 301-303.

[42] R. D. Shannon, Revised effective ionic radii and systematic studies of interatomic distances in halides and chalcogenides, *Acta Crystallographica* A32 (1976) 751-767.

[43] H. Nagata and T. Takenaka, Effects of substitution on electrical properties of $(Bi_{1/2}Na_{1/2})TiO_3$-based lead-free ferroelectrics, *IEEE. Xplore.*

[44] M. Aparna, T. Bhimasankaram, S. V. Suryanaranana, G. Prasad, G. S. Kumar, Effect of lanthanum doping on electrical and electromechanical properties of $Ba_{1-x}La_xTiO_3$, *Bulletin Materials Science* 24 (2001) 497-504.

[45] M. H. Lin, H. Y. Lu, Densification retardation in the sintering of $La_2O_3$ – doped barium titanate ceramic*, Materials Science and Engineering* A323 (2002) 167-176.

[46] P. Siriprapa, A. Watcharapasorn, S. Jiansirisomboon, Effect of La-doped of phase, microstructure and dielectric properties of $Bi_4Ti_3O_{12}$ ceramics, *Advanced Materials* 93-94 (2010) 251-254.

[47] P. Siriprapa, A. Watcharapasorn, S. Jiansirisomboon, Electrical and mechanical characteristics of $(Bi_{4-x}La_x)Ti_3O_{12}$, *Ferroelectrics* 382 (2009) 1-6.

[48] S. Chopra, S. Sharma, T. C. Goel, R. G. Mendiratta, Structural dielectric and ferroelectric properties of La doped $PbTiO_3$ sol gel derived thin films, *Ferroelectrics* 327 (2005) 97-101.

[49] T. Yu, K.W. Kwok, H. L.W. Chan, Preparation and properties of Sol–Gel-derived $Bi_{0.5}Na_{0.5}TiO_3$ lead-free ferroelectric thin film, *Thin Solid Films* 515 [7–8] (2007) 3563-3566.

[50] H. Nagata and T. Takenaka, Effects of substitution on electrical properties of $(Bi_{1/2}Na_{1/2})TiO_3$-based lead-free ferroelectrics, *IEEE. Xplore.*

[51] E. Brzozowski, M.S. Castro, Grain growth control in Nb-doped $BaTiO_3$, *Journal of Materials Processing Technology* 168 (2005) 464-470.

[52] B.-J. Chu, J.-H. Cho, Y.-H. Lee, B.-I. Kim, D.-R. Chen, The potential application of BNT based ceramics in large displacement actuation, *Journal of Ceramics Processing Research* 3 (2002) 231-243.

[53] Liu C, Lan Z, Jiang X, Yu Z, Sun K, Li L, Liu P (2008), Effect of sintering temperature and $Bi_2O_3$ content on microstructure and magnetic properties of LiZn ferrites. *J Magn Magn Mater* 320, 1335–39.

[54] Bomlai, P., Wichianrat, P., Muensit, S. and Steven, J. M. 2007. Effect of calcinations and excess alkali carbonate on the phase formation and particle morphology of $Na_{0.5}K_{0.5}Nb_{0.5}O_3$ powders. *Journal of American Ceramic Society.* 90: 1650-1655.

[55] M. V. Makarova, P. E. Kazin, D. D. Zaitsev, N. S. Eremina, Y. D. Tretyakov and M. Jansen: Preparation of Submicron Strontium Sodium Zirconate Powder in Alkaline Solutions *Inorganic Materials*. Vol. 39 (5) (2003), p. 514-519

[56] W.D.Kingery, H.K.Bowen, D.R.Uhlmann, *Introduction to Ceramic*, 2nd., Jhon wiley & Sons,Inc, New York 1960

[57] Y. Qu, D. Shan and J. Song, Effect of A-site substitution on crystal component and dielectric properties in $Bi_{0.5}Na_{0.5}TiO_3$ ceramics, *Materials Science Eng*lish, 121 (2005) 148.

# Output จากโครงการวิจัยที่ได้รับทุนจาก สกอ. และ สกว.

## 1. ผลงานตีพิมพ์ในวารสารวิชาการและการนำเสนอผลงานในการประชุมวิชาการ

### 1.1 การผลงานตีพิมพ์ในวารสารวิชาการระดับนานาชาติ (ดูภาคผนวก)

1. P. Jaiban, S. Jiansirisomboon, **A. Watcharapasorn**, Effect of lanthanum substitution on microstructure and electrical properties of $(Bi_{0.5}Na_{0.5})_{1-1.5x}La_xTi_{0.41}Zr_{0.59}O_3$ ceramics, accepted to be published in *Ceramics International*. Impact Factor = 1.686

2. A. Rachakom, S. Jiansirisomboon, **A. Watcharapasorn**, Physical and Electrical Properties of Nb doped $Bi_{0.5}Na_{0.5}[Zr_{0.59}Ti_{0.41}]O_3$, accepted to be published in *Ceramics International*. Impact Factor = 1.686

3. **A. Watcharapasorn**, P. Siriprapa, S. Jiansirisomboon, Grain growth behavior in bismuth titanate based ceramics. *Journal of the European Ceramics Society* 30 (2010) 87-93. Impact factor = 1.562)
4. **A. Watcharapasorn**, S. Jiansirisomboon, Dielectric and Piezoelectric Properties of Zirconium-Doped Bismuth Sodium Titanate Ceramics, *Advanced Materials Research* 55-57 (2008) 133-136

### 1.2 การผลงานตีพิมพ์ในวารสารวิชาการระดับชาติ (ดูภาคผนวก)

1. P. Jaiban, S. Jiansirisomboon, **A. Watcharapasorn**, Synthesis of Lead-free $Bi_{0.5}Na_{0.5}ZrO_3$ powder, Journal of Matals, Materials and Minerals, 20(2010) 141-144
2. A. Rachakom, S.Jiansirisomboon, **A. Watcharapasorn**, Microstructures and Mechanical Properties of Lead-Free Bismuth Sodium Titanate Zirconate Ceramics, Journal of Microscopy of Thailand 23, 1 (2009) 107-110.

**1.3 การนำเสนอผลงานในการประชุมวิชาการระดับนานาชาติ (ดูภาคผนวก)**

1. P. Jaiban, A. Rachakom, N. Petnoi, S. Buntham, S. Jiansirisomboon, **A. Watcharapasorn**, Preparation of Bismuth Sodium Zirconate Powder by Mixed-Oxide method, The 12th International Symposium on Eco-Materials Processing and Design, The empress Hotel, Chiang Mai, Thailand, 8-11 January (2011).
2. A. Rachakom, P. Jaiban, N. Petnoi, S. Jiansirisomboon, **A. Watcharapasorn**, Investigation of Morphotropic Phase Boundary for $Bi_{0.5}Na_{0.5}Ti_{1-x}Zr_xO_x$ Solid Solutions by X-ray Diffraction Technique. The 12th International Symposium on Eco-Materials Processing and Design, The empress Hotel, Chiang Mai, Thailand, 8-11 January (2011).
3. P. Jaiban, S. Jiansirisomboon, **A. Watcharapasorn**, Effect of lanthanum substitution on microstructure and electrical properties of $(Bi_{0.5}Na_{0.5})_{1-1.5x}La_xTi_{0.41}Zr_{0.59}O_3$ ceramics, The 7th Asian Meeting on Ferroelectricity and 7th Asian Meeting on Electroceramics (AMF-AMEC-2010), Ramada Plaza Jeju Hotel, Jeju, Korea, 28 June – 1 July (2010).
4. A. Rachakom, S. Jiansirisomboon, **A. Watcharapasorn**, Physical and Electrical Properties of Nb doped $Bi_{0.5}Na_{0.5}[Zr_{0.59}Ti_{0.41}]O_3$, The 7th Asian Meeting on Ferroelectricity and 7th Asian Meeting on Electroceramics (AMF-AMEC-2010), Ramada Plaza Jeju Hotel, Jeju, Korea, 28 June – 1 July (2010)

**1.4 การนำเสนอผลงานในการประชุมวิชาการระดับชาติ (ดูภาคผนวก)**

1. P. Jaiban, A. Rachakom, P. Petnoi, S. Jiansirisomboon, **A. Watcharapasorn**, Effect of Sintering Temperature on Preparation of BNZ ceramics, The 28th Annual conference of the Microscopy Society of Thailand, Mae Fah Luang University, Chiang Rai, Thailand, 5-7 January 2011

2. A. Rachakom, P. Jaiban, S. Jiansirisomboon, **A. Watcharapasorn**, Characteriistics of Nb doped $Bi_{0.5}Na_{0.5}Ti_{0.41}Zr_{0.59}O_3$ ceramics, The 28th Annual conference of the Microscopy Society of Thailand, Mae Fah Luang University, Chiang Rai, Thailand, 5-7 January 2011

3. P. Jaiban, S. Jiansirisomboon, **A. Watcharapasorn**, Synthesis of Lead-free $Bi_{0.5}Na_{0.5}ZrO_3$ powder, The 6th Thailand Materials Science and Technology Conference (MSAT6), Miracle Grand Convention Hotel, Bangkok, Thailand, 26-27 August (2010).

4. A. Rachakom, P. Jaiban, S. Jiansirisomboon, **A. Watcharapasorn**, Effect of calcination time on phase formation of $Bi_{0.5}Na_{0.5}Ti_{1-x}Zr_xO_3$, The 36th Congress on Science and Technology of Thailand, Faculty of Science, Bangkok International Trade and Exhibition Center (BITEC), Bangkok, Thailand, 26 -28 October (2010).

5. P. Jaiban, A. Rachakom, S. Jiansirisomboon, **A. Watcharapasorn**, Effects of calcination temperature and excess $Na_2CO_3$ on phase characteristics of bismuth sodium zirconate powder, The 36th Congress on Science and Technology of Thailand, Faculty of Science, Bangkok International Trade and Exhibition Center (BITEC), Bangkok, Thailand, 26 -28 October (2010).

6. P. Jaiban, A. Rachakom, S. Jiansirisomboon, **A. Watcharapasorn**, Fabrication of lead-free bismuth sodium zirconate ceramics, The 35th Congress on Science and Technology of Thailand, Burapha University, Bang Saean beach, Chonburi, 15 - 17 October 2009.

7. A. Rachakom, P. Jaiban, S. Jiansirisomboon, **A. Watcharapasorn**, Physical and dielectric properties of lead-free bismuth sodium titanate zirconate ceramics, The 35th Congress on Science and Technology of Thailand, Burapha University, Bang Saean beach, Chonburi, 15 - 17 October 2009.

8. A. Rachakom, S. Jiansirisomboon, **A. Watcharapasorn**, Microstructures and mechanical properties of lead-free bismuth sodium titanate zirconate ceramics, The 26th Annual Conference of the Microscopy Society of Thailand, Chiang Mai, Thailand, 28-30 January (2009).

**2. การนำผลงานไปใช้ประโยชน์**

2.1 สามารถสร้างงานวิจัยใหม่ที่น่าสนใจและช่วยให้เกิดการพัฒนาการวิจัยด้านการศึกษาโครงสร้างผลึกเชิงลึกของวัสดุเฟร์โรอิเล็กทริกเซรามิกไร้สารตะกั่วในประเทศไทยได้

2.2 สามารถใช้งานวิจัยนี้เป็นส่วนหนึ่งของการเรียนการสอนในสาขาวิชาวัสดุศาสตร์ ภาควิชาฟิสิกส์ คณะวิทยาศาสตร์ มหาวิทยาลัยเชียงใหม่

2.3 สามารถผลิตผลงานวิจัยเพื่อนำเสนอและแลกเปลี่ยนผลงานวิจัยในการประชุมวิชาการในระดับชาติและนานาชาติได้

2.4 สามารถผลิตบัณฑิตในระดับปริญญาตรี เป็นจำนวน 3 คน ปริญญาโท 1 คน ภายในระยะเวลาสามปีที่ดำเนินโครงการ

2.5 การสร้างเครือข่ายและความร่วมมือในการทำวิจัยกับคณาจารย์และนักวิจัยภายในสถาบันและหน่วยงานต่างๆนอกสถาบันได้

**3. การนำผลงานไปใช้ประโยชน์ด้านอื่น ๆ**

3.1 ได้นำเสนอในการประชุมวิชาการนาโนเทคโนโลยีแห่งประเทศไทย ครั้งที่ 1 เรื่อง วัสดุนาโน เภสัชภัณฑ์ อุปกรณ์ และการประยุกต์ ใช้ ณ โรงแรมเซ็นทรัลดวงตะวัน จังหวัดเชียงใหม่ 14-16 สิงหาคม 2550

Anucha Watcharapasorn and Sukanda Jiansirisomboon ในหัวข้อเรื่อง Effects of $Al_2O_3$ Nano-particle Addition on Electrical and Mechanical Properties of PLZT Ceramics.

3.2 ได้นำเสนอในการประชุมวิชาการ International Conference on Smart Materials: Smart/Intelligen Materials and Nanotechnology and 2$^{nd}$ International Workship on Functional Materials and Nanomaterials, Chiang Mai, Thailand, 22-25 April 2008

A. Watcharapasorn and S. Jiansirisomboon ในหัวข้อเรื่อง Dielectric and Piezoelectric Properties of Zr-doped Bismuth Sodium Titanate Ceramics

# ภาคผนวก

**ผลงานตีพิมพ์ในวารสารวิชาการนานาชาติ**

Gmail by Google

anucha watcharapasorn <anucha.watcharapasorn@gmail.com>

# Request Final Manuscript_2e-P03

**Publication Committee <7th.amec@gmail.com>** **Fri, Jan 7, 2011 at 9:21 AM**
To: "Dr. A.Watcharapasorn" <anucha@stanfordalumni.org>

Dear Dr. A.Watcharapasorn:

We are pleased to inform you that your manuscript entitled, "Effect of lanthanum substitution on microstructure and electrical properties of titanium doped BNZ based ceramics" (2e-P03) has been accepted for publication in the proceedings of AMEC-7, *Ceramics International*.

Although we announced the accepted papers will be published with page charges by authors, your page charges will be covered by the organizing committee of AMEC-7 if some editorial works will be given by each author due to the tight budget for page charges.

We would deeply appreciate it if you could check once again your manuscript in accordance with **Editorial Tips** attached. Especially, be sure to paper length; maximum 4 printed pages allowed for contributed authors and 6 printed pages allowed for invited authors**. Your manuscript will not be included in the Proceedings of AMEC-7 if any editorial faults and any deception for paper length were found in final manuscript.**

Due to the tight schedule of publication process, we strongly ask your **Final Manuscript (Only one MS-Word file including Tables and Figures) with Final Paper Length form** before **January 10, 2011** to Publication Committee of AMEC-7 (**7th.amec@gmail.com**)

IMPORTANT: Any changes other than minor ones such as corrections for typos or English for your accepted manuscript are not allowed. In case more significant corrections or changes are necessary, please submit your modified manuscript to me for review as early as possible with a clear indication where the changes are made so that I may grant final approval. Late changes may incur a heavy editorial cost and should therefore be avoided as much as possible.

Sincerely,
Publication Committee
AMEC-7

Final manuscript

# Effect of lanthanum substitution on microstructure and electrical properties of $(Bi_{0.5}Na_{0.5})_{1-1.5x}La_xTi_{0.41}Zr_{0.59}O_3$ ceramics

Panupong Jaiban [a], Sukanda Jiansirisomboon [a, b], Anucha Watcharapasorn [a, b]*

[a] *Department of Physics and Materials Science, Faculty of Science, Chiang Mai University, Chiang Mai 50200, Thailand*

[b] *Materials Science Research Center, Faculty of Science, Chiang Mai University, 50200 Chiang Mai, Thailand*

* Corresponding author. Tel.: +66-53-94-1921 ext 631; fax: +66-53-94-3445.

*E-mail address:* anucha@stanfordalumni.org (A. Watcharapasorn).

## Abstract

Bismuth sodium zirconate (BNZ) based ceramics with a composition of $(Bi_{0.5}Na_{0.5})_{1-1.5x}La_xTi_{0.41}Zr_{0.59}O_3$ where x = 0, 0.005, 0.01, 0.02 and 0.03 were prepared by a solid-state mixed oxide method and sintered at the temperature of 900°C for 2 h. All the samples had relative density between 91 -97% of their theoretical values. Phase analysis using X-ray diffraction indicated single rhombohedral or pseudo-cubic perovskite structure. SEM micrographs showed that addition of La caused the average grain size of the BNTZ ceramics to decrease as well as an improvement of sample density. Dielectric properties at room temperature measured at 10 kHz indicated that addition of La increased the dielectric constant. The results of ferroelectric characterization also revealed that adding La caused a decrease in coercive field without affecting the remanent polarization.

*Keywords:* D. BLNZT; C. Electrical properties; C. Dielectric properties; D. Perovskites

Gmail by Google

anucha watcharapasorn <anucha.watcharapasorn@gmail.com>

# Request Final Manuscript_2e-P02

**Publication Committee <7th.amec@gmail.com>** **Fri, Jan 7, 2011 at 9:17 AM**
To: "Dr. A.Watcharapasorn" <anucha@stanfordalumni.org>

Dear Dr. A.Watcharapasorn:

We are pleased to inform you that your manuscript entitled, "Physical and Electrical properties of Nb doped $Bi_{0.5}Na_{0.5}[Zr_{0.59}Ti_{0.41}]O_3$" (2e-P02) has been accepted for publication in the proceedings of AMEC-7, *Ceramics International*.

Although we announced the accepted papers will be published with page charges by authors, your page charges will be covered by the organizing committee of AMEC-7 if some editorial works will be given by each author due to the tight budget for page charges.

We would deeply appreciate it if you could check once again your manuscript in accordance with **Editorial Tips** attached. Especially, be sure to paper length; maximum 4 printed pages allowed for contributed authors and 6 printed pages allowed for invited authors**. Your manuscript will not be included in the Proceedings of AMEC-7 if any editorial faults and any deception for paper length were found in final manuscript.**

Due to the tight schedule of publication process, we strongly ask your **Final Manuscript (Only one MS-Word file including Tables and Figures) with Final Paper Length form** before **January 10, 2011** to Publication Committee of AMEC-7 (**7th.amec@gmail.com**)

IMPORTANT: Any changes other than minor ones such as corrections for typos or English for your accepted manuscript are not allowed. In case more significant corrections or changes are necessary, please submit your modified manuscript to me for review as early as possible with a clear indication where the changes are made so that I may grant final approval. Late changes may incur a heavy editorial cost and should therefore be avoided as much as possible.

Sincerely,
Publication Committee
AMEC-7

Revised manuscript - Highlighted

# Physical and Electrical Properties of Nb doped $Bi_{0.5}Na_{0.5}[Zr_{0.59}Ti_{0.41}]O_3$

Ampika Rachakom[a], Sukanda Jiansirisomboon[a,b], Anucha Watcharapasorn[a,b*]

[a] *Department of Physics and Materials Science, Faculty of Science,*

*Chiang Mai University, 50200 Chiang Mai, Thailand*

[b] *Materials Science Research Center, Faculty of Science, Chiang Mai University,*

*50200 Chiang Mai, Thailand*

**Corresponding author.* Tel.: +66 53 941 921x632; fax: +66 53 892 271.

*E-mail address:* anucha@stanfordalumni.org (A. Watcharapasorn).

**Abstract**

This research studied the effect of Nb doping on $Bi_{0.5}Na_{0.5}[Ti_{0.41}Zr_{0.59}]O_3$ (when Nb concentration = 0.00, 0.01, 0.03, 0.05, 0.07 and 0.09 mole fraction). Nb doped BNTZ ceramics were fabricated using a conventional mixed-oxide method. All samples were calcined at a temperature of 700 ºC for 2 h and sintered at a temperature of 900 ºC for 2 h. X-ray diffraction patterns suggested that the compounds possessed rhombohedral perovskite structure. SEM micrographs indicated that average grain size decreased as the amount of Nb additives increased. The electrical resistivity showed a decreasing trend with increasing Nb concentration due to excess charge present in the sample. The

dielectric constant and dielectric loss of samples showed no particular trend when Nb was added but the optimum was observed when 0.05-0.07 Nb mole fraction was present in BNTZ ceramics. In this study, both microstructure and donor-type effects played an important role in determining electrical resistivity and dielectric properties of these ceramics.

*Keywords:* D. Bismuth sodium titanate; B. X–ray method; C. Dielectric properties; C. Electrical properties.

Available online at www.sciencedirect.com
ScienceDirect
Journal of the European Ceramic Society 30 (2010) 87–93
www.elsevier.com/locate/jeurceramsoc

# Grain growth behavior in bismuth titanate-based ceramics

A. Watcharapasorn, P. Siriprapa, S. Jiansirisomboon *

*Department of Physics and Materials Science, Faculty of Science, Chiang Mai University, Chiang Mai 50200, Thailand*

Received 3 April 2009; received in revised form 29 July 2009; accepted 30 July 2009
Available online 28 August 2009

**Abstract**

Bismuth titanate and lanthanum-doped bismuth titanate ceramics were prepared from freeze-dried powders employing conventional solid state reaction and sintering procedures. The sintering process was carried out at 1150 °C from 4 up to 48 h. X-ray diffraction analysis showed that preferred orientation was reduced in bismuth titanate ceramic as sintering time increased while lanthanum-doped sample showed much less degree of preferred orientation and was independent of sintering time. Grain growth studies also showed that initial anisotropic grain growth rate was the main factor controlling the grain morphology, rendering the plate-shaped grain in both pure and lanthanum-doped bismuth titanate ceramics. Based on established grain growth law, pore-controlled diffusion could be the major mechanism determining the observed microstructure in these layered compounds.


*Keywords:* Sintering; Grain growth; Powders-solid state reaction; Bismuth titanate-based compound

## 1. Introduction

Pure and doped bismuth titanate ($Bi_4Ti_3O_{12}$ or BIT) have been under investigation recently due to their good electrical fatigue resistance behavior and their possible use in ferroelectric random access memories or FRAM applications.[1] A number of techniques have been employed to synthesize these materials both in thin film and ceramic forms.[2–6] For thin films, a number of research work have shown that highly *c*-axis oriented grain morphology could be produced by several processing techniques particularly the templated grain growth method which enabled measurements of anisotropic properties of these films.[7–10]

In ceramics, it has been well known that both pure and doped BIT possess plate-like grains and properties which are also orientation dependent. For example, dielectric properties along the direction perpendicular and parallel to *c*-axis were found to be quite different.[11] Hence, due to anisotropic behavior of this material, a number of researchers have fabricated BIT ceramics with grains aligned in certain direction by various techniques such as templated grain growth and tape-casting.[12] Others have found that employing external parameters such as magnetic field or pressure could also produce ceramics with oriented grains.[11–14] Inoue et al.[12] had shown that BIT ceramics with highly oriented grains could be fabricated from compacted plate-shaped powders which were originally prepared from salt solutions. However, the prepared ceramics contained large pores between well sintered plate-shaped grain colonies.[12] The authors also briefly mentioned the anisotropic grain growth behavior of sintered green compact prepared from conventionally prepared BIT powder. Based on these previous studies and the fact that grain growth kinetics and time dependence of grain morphology of BIT ceramics prepared by conventional sintering method have not been investigated in detail, this research therefore attempts to quantitatively study the effects of sintering time on microstructures, grain orientation and density of BIT ceramics. The results are discussed and compared to those of $Bi_{3.25}La_{0.75}Ti_3O_{12}$ (BLT) ceramics to elucidate the effects of lanthanum ion addition on grain growth behavior of BIT ceramics.

## 2. Experimental procedure

$Bi_4Ti_3O_{12}$ and $Bi_{3.25}La_{0.75}Ti_3O_{12}$ powders were prepared from binary oxides i.e. $Bi_2O_3$ (>98.0%, Fluka), $La_2O_3$ (99.99%, Cerac) and $TiO_2$ (>99%, Riedel-de Haën). The stoichiometric amounts of starting powders were mixed using ball milling with

* Corresponding author. Tel.: +66 53 941921x631; fax: +66 53 943445.
*E-mail address:* sukanda@chiangmai.ac.th (S. Jiansirisomboon).

0955-2219/$ – see front matter © 2009 Elsevier Ltd. All rights reserved.
doi:10.1016/j.jeurceramsoc.2009.07.031

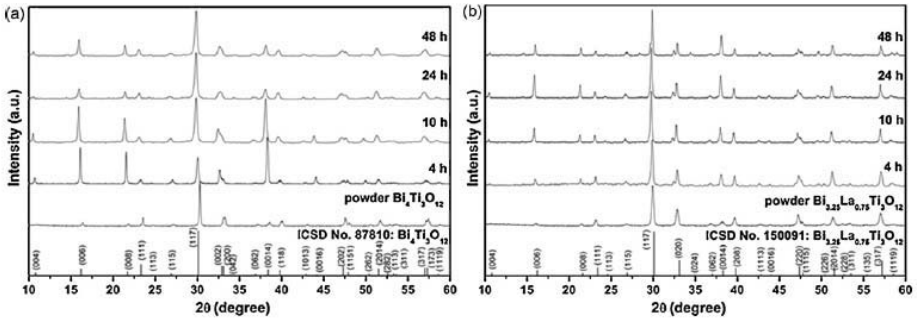


Fig. 1. X-ray diffraction patterns of calcined powder and sintered ceramics of (a) $Bi_4Ti_3O_{12}$ and (b) $Bi_{3.25}La_{0.75}Ti_3O_{12}$.

zirconia balls and distilled water for 24 h at a rate of 60 rpm. The mixtures were then transferred to a spherical flask and placed in a shell freezer. The flask was rotated in an ethanol bath for at least 1 h to produce frozen slurry, which was immediately dried in a vacuum drier for at least 24 h. After all ice was sublimated, fine freeze-dried powders were obtained. The powders were then calcined at 750 °C for 4 h before being re-ground, pressed into small pellets and sintered at 1150 °C for 4, 10, 24 and 48 h. X-ray diffraction analysis was employed to study phase formation and crystal structure of calcined powder and polished surfaces of ceramics using an X-ray diffractometer (Philips model X-pert) with $CuK_\alpha$ radiation. Density was measured using Archimedes method. Microstructure of ceramic surfaces thermally etched in air at 1000 °C for 15 min was investigated using a scanning electron microscope (JEOL JSM-6335F). Grain size was obtained from SEM micrographs using direct measurement of grain length and thickness across the center of each grain. Averaged values for each sample were obtained from measuring one hundred grains. For degree of grain orientation, the following equations were used

$$P_0 = \frac{\sum I_0(0\,0\,l)}{\sum I_0(h\,k\,l)} \quad (1)$$

$$P = \frac{\sum I(0\,0\,l)}{\sum I(h\,k\,l)} \quad (2)$$

In the above equations, $P_0$ and $P$ are the fraction of $(0\,0\,l)$ X-ray peaks with respect to all peaks for powders and ceramics, respectively. $I_0(0\,0\,l)$ and $I(0\,0\,l)$ are the integrated X-ray $0\,0\,l$ peak intensities of powder and ceramic samples, respectively. $I_0(h\,k\,l)$ and $I(h\,k\,l)$ are their corresponding integrated intensities of all peaks within the $2\theta$ range (i.e. 10–60°) under investigation. After $P_0$ and $P$ were calculated, a Lotgering factor[15] was obtained using equation

$$F = \frac{P - P_0}{1 - P_0} \quad (3)$$

## 3. Results and discussion

Fig. 1(a) shows X-ray diffraction patterns of BIT ceramics. For sintering time of 4 h, the ceramic surface showed relatively high degree of preferred orientation of $0\,0\,l$-type indices. As the sintering time increased, the degree of preferred orientation decreased. Quantitatively, the $0\,0\,l$-oriented grain contribution approximated from integrated intensity of X-ray peaks relative to other grain orientation is also shown in Fig. 2. It seems therefore that for short sintering time (4 and 10 h), the compacted particles with $c$-axis oriented parallel to the pressing direction tended to grow and contribute to high degree of $0\,0\,l$ preferred orientation observed. At longer sintering time (24 and 48 h), the influence of grains with $c$-axis oriented perpendicular to pressing direction became more pronounced (Fig. 1(a)) with a corresponding reduction in $0\,0\,l$ preferred orientation (Fig. 2). These grains seemed to grow over some of the $0\,0\,l$-oriented grains, hence rendering smaller fraction of the latter on the ceramic surface. It should be noted that a slight shift of X-ray peaks of BIT ceramics compared to that of powder was probably due to instrumental error since the weight loss during sintering was found to be negligible, indicating that stoichiometry did not change and, therefore, X-ray patterns of ceramics and powder should be identical.

Fig. 1(b) shows X-ray diffraction of BLT calcined powder and sintered ceramics. Although the X-ray pattern of calcined

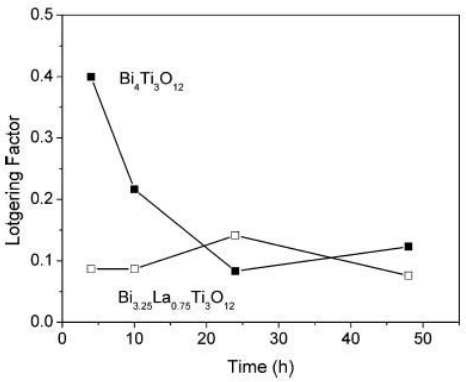


Fig. 2. Lotgering factor as a function of sintering time for BIT and BLT ceramics with respect to their calcined powders.

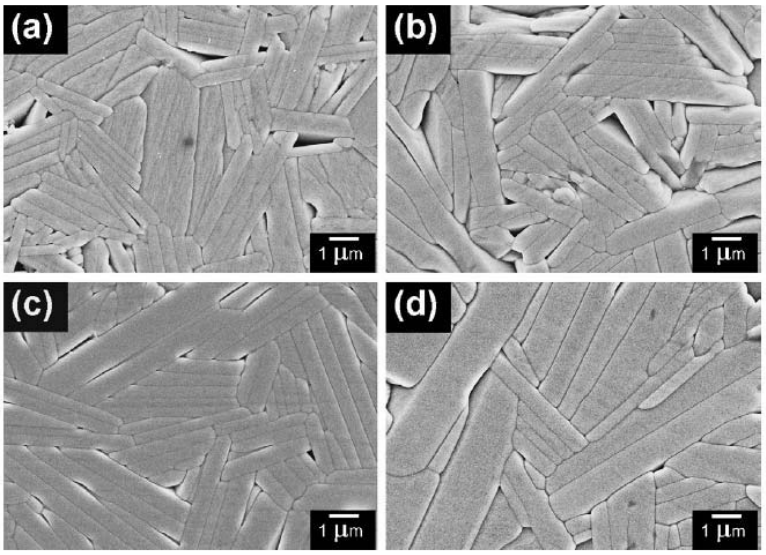


Fig. 3. SEM micrographs of thermally etched surfaces of BIT ceramics at various sintering times: (a) 4 h, (b) 10 h, (c) 24 h and (d) 48 h.

BLT powder was nearly the same as that of BIT, it could be seen that the degree of 0 0 *l* preferred orientation of BLT ceramics was much less than that of BIT ceramics when compared at the same sintering time. The effect of sintering time on degree of preferred orientation based on calculated Lotgering factor of 0 0 *l*-oriented grains is also shown in Fig. 2. It could be seen that, compared to BIT ceramics, the degree of grain orientation of BLT was nearly independent of sintering time. For long sintering period, the degree of 0 0 *l*-type preferred orientation in BIT and BLT ceramics was nearly the same. This suggested that the grain

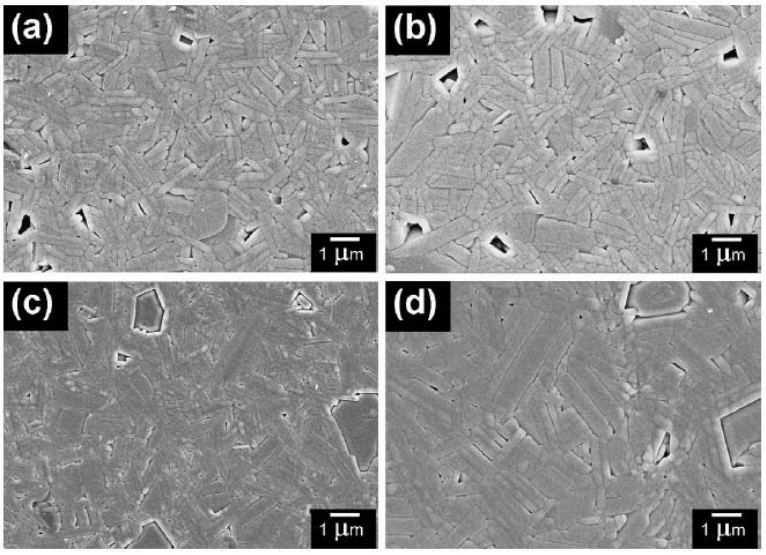


Fig. 4. SEM micrographs of thermally etched surfaces of BLT ceramics at various sintering times: (a) 4 h, (b) 10 h, (c) 24 h and (d) 48 h.

Table 1
Grain length and thickness of $Bi_4Ti_3O_{12}$ and $Bi_{3.25}La_{0.75}Ti_3O_{12}$.

| Sintering time (h) | Grain length: $l$ (μm) | | Grain thickness: $t$ (μm) | | $l/t$ | |
|---|---|---|---|---|---|---|
| | BIT | BLT | BIT | BLT | BIT | BLT |
| 4 | 5.88 ± 1.99 | 2.15 ± 0.73 | 0.98 ± 0.30 | 0.54 ± 0.13 | 6.00 | 3.98 |
| 10 | 8.44 ± 2.58 | 2.33 ± 0.66 | 1.46 ± 0.46 | 0.62 ± 0.16 | 5.78 | 3.74 |
| 24 | 9.62 ± 3.96 | 2.81 ± 1.00 | 1.67 ± 0.57 | 0.63 ± 0.15 | 5.76 | 4.45 |
| 48 | 10.38 ± 4.82 | 3.01 ± 1.21 | 1.77 ± 0.64 | 0.73 ± 0.21 | 5.86 | 4.12 |

Table 2
Density of $Bi_4Ti_3O_{12}$ and $Bi_{3.25}La_{0.75}Ti_3O_{12}$ ceramics.

| Sintering time (h) | $Bi_4Ti_3O_{12}$ | | $Bi_{3.25}La_{0.75}Ti_3O_{12}$ | |
|---|---|---|---|---|
| | Density (g/cm$^3$) | Relative density[a] (%) | Density (g/cm$^3$) | Relative density[a] (%) |
| 4 | 7.55 ± 0.01 | 94.15 | 7.40 ± 0.03 | 96.47 |
| 10 | 7.41 ± 0.08 | 92.40 | 7.43 ± 0.02 | 96.88 |
| 24 | 7.31 ± 0.01 | 91.14 | 7.44 ± 0.03 | 96.95 |
| 48 | 7.38 ± 0.01 | 92.00 | 7.17 ± 0.13 | 93.51 |

[a] X-ray density of $Bi_4Ti_3O_{12}$ = 8.02 g/cm$^3$ and $Bi_{3.25}La_{0.75}Ti_3O_{12}$ = 7.67 g/cm$^3$.

growth kinetics of these two systems might be similar at long sintering time.

Figs. 3 and 4 show thermally etched surfaces of BIT and BLT ceramics, respectively. For the same sintering time, the grain size of BIT was much larger than that of BLT ceramic. As the sintering time increased, the grain size became increased both in terms of grain length and thickness. Their values are listed in Table 1. The density for both compounds did not vary much with sintering time (see Table 2). It could be observed however that the relative density of BIT ceramics was slightly less than that of BLT due to the larger plate-like grains, causing greater difficulties in having high packing density. Their low density values were also confirmed in the micrographs in which relatively high fraction of large pores was observed in BIT compared to that of BLT ceramics.

To study grain growth behavior in these compounds, the grain size in terms of grain length and thickness as a function of time was plotted and shown in Fig. 5. It could be observed that, in both BIT and BLT ceramics, the grain size along *ab*-plane initially increased abruptly and then increased more slowly at longer sintering time. Regardless of sintering time, both grain length and thickness of BIT ceramics were much larger than that of BLT ceramics. This indicates the well known effect of grain growth inhibition by lanthanum ions. To further quantify this point, the grain growth rate was obtained by fitting an empirical curve to the data points. It was found that the best fitted curve was obtained using the power function in the form $G = abt^{1-c}/(1 + bt^{1-c})$, where $G$ is the grain size (length or thickness), $t$ is the time, and $a$, $b$, $c$ are the fitting constants. After the fitting, the slope was calculated to obtain instantaneous grain growth rate.

Fig. 6 shows the growth rate as a function of sintering time. It is apparent that the initial growth rate along *ab*-plane (grain length) was much faster than that along *c*-axis (grain thickness) for both BIT and BLT ceramics. This grain growth anisotropy could be largely due to the different atomic attachment/diffusion

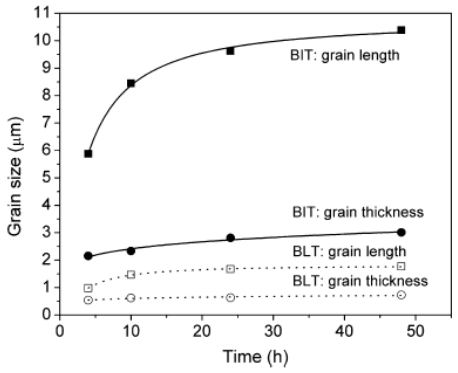


Fig. 5. Grain size of BIT and BLT ceramics as a function of sintering time.

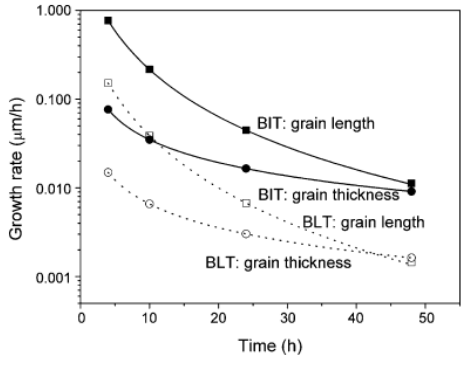


Fig. 6. Grain growth rate of BIT and BLT ceramics as a function of sintering time.

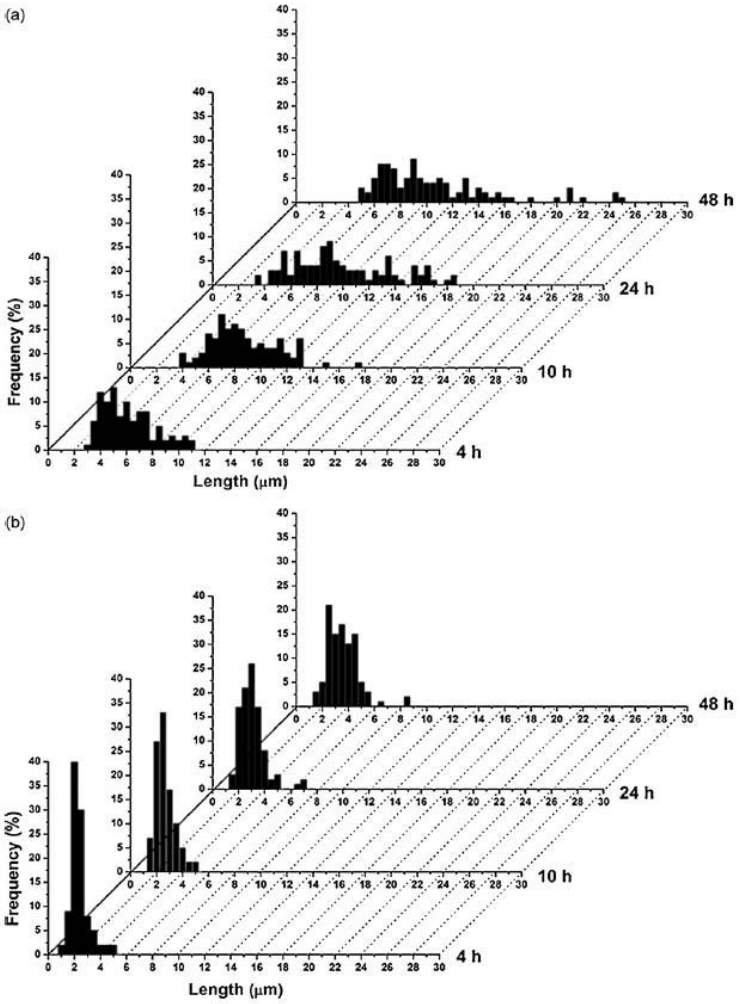


Fig. 7. Grain size distribution as a function of sintering time: (a) BIT and (b) BLT ceramics.

rates along different directions which, in turn, were influenced by the orthorhombic crystal structure of BIT and BLT. From the figure, it could be observed that the grain growth rate of BIT ceramic in both directions was about 10 times faster than that of BLT ceramic. This further proved the effectiveness of lanthanum in grain growth inhibition. As the sintering time increased, the growth rates in both directions decreased until their values became comparable at long sintering time. This reduction in grain growth rate should be expected since as the grain grew, more time would be needed to complete each atomic layer on each grain. This comparable grain growth along *ab*-plane and *c*-axis at long sintering time in both BIT and BLT ceramics also seemed to play a large part in determining the amount of preferred orientation in these ceramics. Hence, the initial anisotropic grain growth rate seemed to be the main factor causing the plate-shaped microstructures in both BIT and BLT ceramics. For long sintering time, the grain growth rate became more isotropic with reduced preferred orientation as observed in this study. The effect of lanthanum on grain growth inhibition also resulted in narrower grain size distribution in BLT ceramics compared to that of BIT ceramics, as shown in Fig. 7.

In terms of grain growth mechanism in BIT and BLT ceramics, attempts to find the values of exponent $m$ in the grain growth law i.e. having a relationship $G^m - G_0^m = kt$,[16] where $G_0$ is grain size at time $t = 0$ and $k$ is a constant, were not very successful. Fig. 8 shows the plot of a straight line fit through data

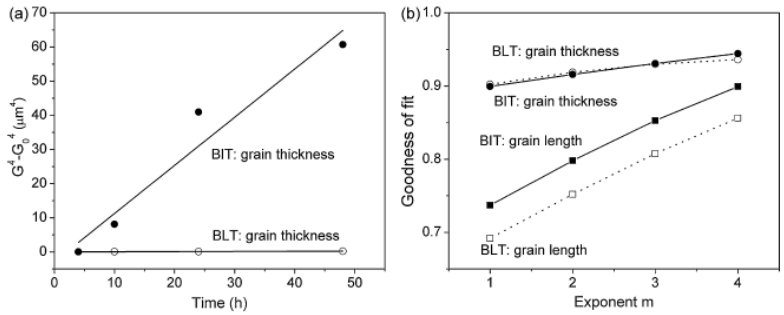


Fig. 8. Grain growth law applied to BIT and BLT ceramics: (a) linear fitting for $m = 4$ and (b) goodness of fit as a function of exponent $m$.

points (using $m = 4$ in this case) and the goodness of fit (having an ideal value of 1) as a function of exponent $m$. It could be seen that the best fit, though still having relatively large residual error, was found for $m$ equals 4 which corresponded to the pore-controlled surface diffusion or boundary-controlled diffusion due to coalescence of second phase.[16] However, the samples investigated in this study were mostly single phase so it was unlikely that the latter mechanism would play much role. Hence, pore-controlled surface diffusion may be a major mechanism in this material. Care should be taken however that other diffusion mechanisms may also play a role in these materials. The difficulties in applying grain growth law to BIT and BLT ceramics were due to the fact that these materials possessed anisotropic grain growth behavior as well as the fact that the grain growth law was established based on the assumption that the material must be a homogeneous compact with isotropic grain boundary energy and isolated spherical pores at the grain boundary. These properties were not closely followed in BIT and BLT ceramics due to their un-equiaxed grains. Nevertheless, based on the information obtained in this study, the rate controlling factors of grain growth could be the interfacial energy as well as the mobility of lanthanum ions. Further detailed investigation of lanthanum ion diffusion in BIT ceramic would be beneficial.

## 4. Conclusions

The $Bi_4Ti_3O_{12}$ and $Bi_{3.25}La_{0.75}Ti_3O_{12}$ ceramics sintered at various sintering times up to 48 h were successfully fabricated. X-ray diffraction analysis showed that while $Bi_4Ti_3O_{12}$ ceramics showed greater 0 0 $l$-type preferred orientation than $Bi_{3.25}La_{0.75}Ti_3O_{12}$ ceramics at short sintering time, both materials had similar degree of 0 0 $l$-type preferred orientation at longer sintering period. In both $Bi_4Ti_3O_{12}$ and $Bi_{3.25}La_{0.75}Ti_3O_{12}$ ceramics, the anisotropic grain growth rate was observed at short sintering period while at long sintering time, the growth rate along *ab*- and *c*-plane became comparable. This study showed that the plate-shaped morphology in $Bi_4Ti_3O_{12}$ and $Bi_{3.25}La_{0.75}Ti_3O_{12}$ ceramics was mainly the results of initial anisotropic grain growth rate. Sintering these ceramics at longer time could render a material with more isotropic microstructure with reduced preferred orientation.

## Acknowledgements

This work is supported by the Thailand Research Fund (TRF), the Commission on Higher Education (CHE), the Faculty of Science and the Graduate School, Chiang Mai University. Ms. Pasinee Siriprapa would like to thank the Commission on Higher Education, Thailand for supporting by grant fund under the program Strategic Scholarships for Frontier Research Network for the Ph.D. Program Thai Doctoral degree for this research.

## References

1. Park, B. H., Kang, B. S., Bu, S. D., Noh, T. W., Lee, J. and Jo, W., Lanthanum-substituted bismuth titanate for use in non-volatile memories. *Nature*, 1999, **401**, 682–684.
2. Simões, A. Z., Quinelato, C., Ries, A., Stojanovic, B. D., Longo, E. and Varela, J. A., Preparation of lanthanum doped $Bi_4Ti_3O_{12}$ ceramics by the polymeric precursor method. *Mater Chem Phys*, 2006, **98**, 481–485.
3. Shen, L., Xiao, D., Zhu, J., Yu, P., Zhu, J. and Gao, D., Study of $(Bi_{4-x}La_x)Ti_3O_{12}$ powders and ceramics prepared by sol–gel method. *J Mater Syn Process*, 2001, **9**, 369–373.
4. Kan, Y., Jin, X., Zhang, G., Wang, P., Cheng, Y. B. and Yan, D., Lanthanum modified bismuth titanate prepared by a hydrolysis method. *J Mater Chem*, 2004, **14**, 3566–3570.
5. Kang, S. W., Song, M. K., Rhee, S. W., Suh, J. H. and Park, C. G., Interface and crystal structures of lanthanum substituted bismuth titanate thin films grown on Si for metal ferroelectric semiconductor structure. *Integr Ferroelectrics*, 2005, **72**, 61–70.
6. Stojanovic, B. D., Simões, A. Z., Paiva-Santos, C. O., Quinelato, C., Longo, E. and Varela, J. A., Effect of processing route on the phase formation and properties of $Bi_4Ti_3O_{12}$ ceramics. *Ceram Int*, 2006, **32**, 707–712.
7. Xiang, P.-H., Kinemuchi, Y. and Watari, K., Preparation of *c*-axis-oriented $Bi_4Ti_3O_{12}$ thick films by templated grain growth. *J Eur Ceram Soc*, 2007, **27**, 663–667.
8. Chon, U., Jang, H. M. and Park, I. W., Ferroelectric properties of highly *c*-axis oriented $Bi_{4-x}La_xTi_3O_{12}$ film-based capacitors. *Solid State Commun*, 2003, **127**, 469–473.
9. Bae, J. C., Kim, S. S., Choi, E. K., Song, T. K., Kim, W. J. and Leed, Y. I., Ferroelectric properties of lanthanum-doped bismuth titanate thin films grown by a sol–gel method. *Thin Solid Films*, 2005, **472**, 90–95.
10. Kan, Y., Wang, P., Li, Y., Cheng, Y.-B. and Yan, D., Fabrication of textured bismuth titanate by templated grain growth using aqueous tape casting. *J Eur Ceram Soc*, 2003, **23**, 2163–2169.
11. Chen, W., Kinemuchi, Y., Tamura, T., Miwa, K. and Watari, K., Preparation of *a*–*b* plane oriented Nb-doped $Bi_4Ti_3O_{12}$ ceramics by magnetic alignment via gelcasting. *Mater Res Bull*, 2006, **41**, 2094–2101.

12. Inoue, Y., Kimura, T. and Yamaguchi, T., Sintering of platelike bismuth titanate powders. *Am Ceram Soc Bull*, 1983, **62**, 704–707.
13. Chen, W., Hotta, Y., Tamura, T., Miwa, K. and Watari, K., Effect of suction force and starting powders on microstructure of $Bi_4Ti_3O_{12}$ ceramics prepared by magnetic alignment via slip casting. *Scripta Mater*, 2006, **54**, 2063–2068.
14. Liu, J., Shen, Z., Nygren, M., Kan, Y. and Wang, P., SPS processing of bismuth-layer structures ferroelectric ceramics yielding highly textured microstructures. *J Eur Ceram Soc*, 2006, **23**, 3233–3239.
15. Lotgering, F. K., Topotactical reactions with ferromagnetic oxides having hexagonal crystal structures. *J Inorg Nucl Chem*, 1959, **9**, 113–123.
16. Rahaman, M. N., *Sintering of ceramics*. CRC Press, Boca Raton, 2008.

*Advanced Materials Research Vols. 55-57 (2008) pp 133-136*
*online at http://www.scientific.net*




# Dielectric and Piezoelectric Properties of Zirconium-Doped Bismuth Sodium Titanate Ceramics

A. Watcharapasorn[a] and S. Jiansirisomboon[b]

Department of Physics, Faculty of Science, Chiang Mai University,
Chiang Mai 50200, Thailand

[a] anucha@stanfordalumni.org, [b] sukanda@chiangmai.ac.th

**Keywords:** BNT, dielectric, piezoelectric, solid solution

**Abstract.** Zirconium-doped bismuth sodium titanate ceramics were prepared using the conventional processing method. X-ray diffraction analysis indicated the materials were single phase with a systematic shift due to increased unit cell size. The measured densities and grain size of the ceramic samples were found to range from 5.79-6.03 g/cm$^3$ and 0.5-1.6 μm, respectively. The dielectric constant as a function of temperature became broader as Zr content increased. The piezoelectric constant was found to decrease with increasing Zr. Within the range of the solid solutions investigated, the materials seem to be promising for high temperature applications where stable dielectric constant is required.

## Introduction

It is well known that a number of solid solution systems in ferroelectric ceramics are scientifically and technologically important. These include $Pb(Zr,Ti)O_3$, $Pb(Mg_{1/3}Nb_{2/3})O_3$-$PbTiO_3$ and $Pb(Zn_{1/3}Nb_{2/3})O_3$-$PbTiO_3$, which have already been widely used in many sensor and actuator applications [1, 2]. However, the lead-containing compounds are currently of environmental concerns for future devices. Therefore, a number of non-lead material systems have been investigated in order to to find suitable replacement for lead-based compounds. One of these non-lead systems is the solid solution of $BaTiO_3$-$BaZrO_3$ (BZT) which was found to possess high dielectric constant, low loss, high-strain capability and large piezoelectric coefficient [3-9].

Besides BZT, bismuth sodium titanate having chemical formula, $Bi_{0.5}Na_{0.5}TiO_3$ or BNT, has recently been received more attention due to their interesting ferroelectric properties. These include remanent polarization of 38 μC/cm$^2$, coercive field of 73 kV/cm and high Curie temperature ($T_c$ = 320 ºC) [10-13]. Although a number of dopants have been used to modify properties of BNT ceramics [13-15], the solid solution $Bi_{0.5}Na_{0.5}(Ti,Zr)O_3$ have not yet been investigated in detail.

In this paper, the effects of Zr concentration on physical, dielectric and piezoelectric properties of BNT are studied and discussed.

## Experimental

$Bi_{0.5}Na_{0.5}Ti_{1-x}Zr_xO_3$ (where x = 0, 0.05, 0.10, 0.15 and 0.20) powders were prepared from binary oxides, i.e. $Bi_2O_3$ (>98%, Fluka ), $Na_2CO_3$ (99.5%, Carlo Erba), $TiO_2$ (>99%, Riedel-de Haën) and $ZrO_2$ (>99%, Fluka). The powder mixtures were ball-milled for 24 h using zirconia milling media in ethanol prior to calcination in alumina crucible at 800 ºC for 2 h. After phase analysis by X-ray diffraction technique (XRD, JDX-8030), the powders were pressed into small pellets and sintered at 1100 ºC for 2 h. The sintered ceramics were characterized for their densities using Archimedes method. The surface morphologies were studied using a scanning electron microscope (JEOL JSM-5910LV) and the grain size was obtained using a linear interception method. The dielectric constant as a function of temperature was measured using an LCR HITESTER connected to a high temperature furnace. The piezoelectric constant was measured using a $d_{33}$-meter (KCF PM-3001) after poling each sample for 5 minutes in 60 ºC silicone oil under 40 kV/cm electric field.

**Results and Discussion**

X-ray diffraction patterns of $Bi_{0.5}Na_{0.5}Ti_{1-x}ZrxO_3$ (BNTZ) calcined powders and sintered ceramics are shown in Fig.1. For samples having the same composition, there was virtually no difference between X-ray patterns of powders and ceramics. The X-ray diffraction pattern of undoped BNT indicated the rhombohedral crystal structure, in agreement with the standard powder diffraction file no. 36-0340 and the pattern reported in literature [13,15]. Incorporation of Zr ions into BNT lattice caused a slight systematic shift of X-ray patterns to the left without changing relative peak intensities which suggested that the rhombohedral structure was maintained while the size of unit cell increased with increasing amount of Zr. Similar increase in lattice parameter was also observed for Zr-doped $BaTiO_3$ due to the larger Zr-ion substitution in $Ti^{4+}$ site [16].

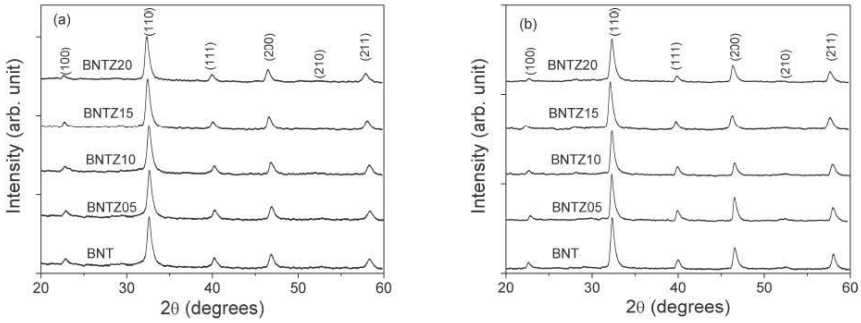


Figure 1. X-ray diffraction patterns of BNTZ: (a) calcined powder and (b) sintered ceramics

The density and the average grain size of BNT and BNTZ ceramics are listed in Table 1. The densities were within the range of 5.79-6.03 $g/cm^3$, corresponding to the relative density of at least 95% of theoretical value. The average grain size ranged from 0.5-1.6 μm and increased with increasing Zr content. This indicated that the addition of $ZrO_2$ did not significantly affect the microstructures of BNTZ ceramics compared with that of BNT.

Table 1. Some room temperature properties of BNTZ ceramics.

| | BNT | BNTZ05 | BNTZ10 | BNTZ15 | BNTZ20 |
|---|---|---|---|---|---|
| Density ($g/cm^3$) | 5.95 | 5.79 | 5.94 | 5.93 | 6.03 |
| Grain size (μm) | 0.5 | 1.0 | 1.1 | 1.2 | 1.6 |
| $d_{33}$ (pC/N) | 68 | 57 | 52 | 47 | 40 |
| $\varepsilon_r$ | 524 | 620 | 655 | 572 | 562 |
| tan δ | 0.06 | 0.04 | 0.04 | 0.04 | 0.05 |

The dielectric constant and dielectric loss plotted as a function of temperature at 10 kHz are shown in Fig. 2. The dielectric curve for BNT showed a normal behavior and had the maximum value at 320 °C, which was the transition temperature commonly found by other researchers [10-15]. The room temperature dielectric constant value of BNT (see Table 1) agreed well with the values reported [13-15]. The room temperature dielectric constant slightly increased with increasing Zr content up to 10 mol%Zr and then decreased with further addtion of Zr. Unlike the $BaTiO_3$-$BaZrO_3$

system [8,9] where addition of Zr decreased the $T_c$ of the ceramics, the effect of Zr on the transition temperature of BNTZ was rather small.

In Fig. 2, it can be seen that increasing Zr concentration caused the dielectric-temperature curves to become more diffused with corresponding lower values of high-temperature dielectric constant. Since no frequency dependence of the dielectric constant was observed (not shown), the amount of Zr used in this study did not render the relaxor behavior of this material. This seems to be in agreement with the study on $BaTiO_3$-$BaZrO_3$ solid solution in which the frequency dependence of the dielectric constant was observed only when the amount of Zr used was equal to or greater then 30 mol% [8,9].

From Fig. 2 (b), except for BNTZ20, the dielectric loss of other BNTZ ceramics showed a relatively constant value for all samples up to about 150 °C. Above this temperature, the values slightly decreased and then increased as the loss became more significant at high temperature. This behavior was also observed in BZT system [8,9]. The room temperature dielectric loss values for BNTZ ceramics were comparable to that of BNT sample. The $d_{33}$ piezoelectric constant of BNTZ showed a decreasing trend with increasing Zr content (see Table 1). It seems therefore that the random distribution of larger Zr ions inside BNT lattice caused some reduction in polarizability of material. It would be interesting, however, to further investigate the BNTZ system in order to find out whether the morphotropic phase boundary is present in order to obtain materials with good dielectric and piezoelectric properties following the PZT and BZT systems.

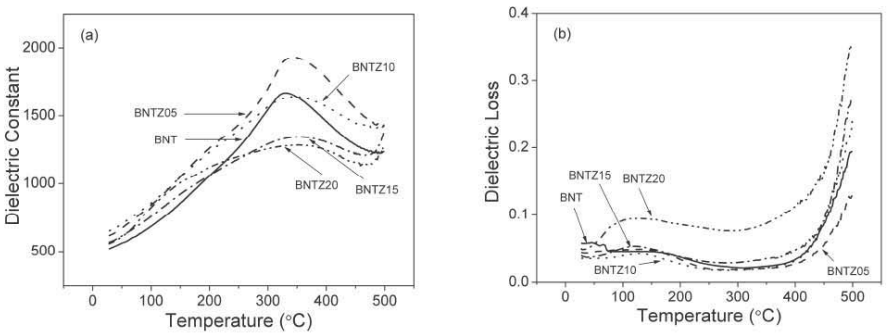


Figure 2. Graph of (a) dielectric constant and (b) dielectric loss of BNTZ ceramics at 10 kHz plotted as a function of temperature.

## Summary

The single-phase $Bi_{0.5}Na_{0.5}Ti_{1-x}Zr_xO_3$ ceramics with x varied from 0 to 0.2 were successfully prepared using conventional ceramic processing method. X-ray diffraction analysis showed a single rhombohedral perovskite phase with systematic shift in peak position, indicating that substitution of $Zr^{4+}$ ions into $Ti^{4+}$ site caused lattice expansion. The piezoelectric coefficient ($d_{33}$) showed a decreasing trend while the dielectric constant-temperature curves showed a broader peak with increasing Zr concentration. This seems to suggest that the material might be used as a high-stability dielectric material.

## Acknowledgments

This work was financially supported by the Thailand Research Fund (TRF), the Commission on Higher Education (CHE) and the National Science and Technology Development Agency (NSTDA). The authors would also like to thank the Faculty of Science, Chiang Mai University

## References

[1] K. Uchino: *Piezoelectric Actuators and Ultrasonic Motors* (Kluwer, Boston 1997).
[2] G.H. Haertling: J. Am. Ceram. Soc. Vol. 82, 4 (1999) p. 797.
[3] P.W. Rehrig, S.E. Park, S.T. McKinstry, G.L. Messing, B. Jones and T.M. Shrout: J. Appl. Phys. Vol. 86 (1999) p.1657.
[4] Y. Zhi, R. Guo and A.S. Bhalla: J. Appl. Phys. Vol. 88 (2000) p. 410.
[5] S.M. Neirman: J. Mater. Sci. Vol. 23 (1988) p. 3973.
[6] J. Ravez and A. Simon: Eur. J. Solid State Inor. Chem. Vol. 34 (1997) p. 1199.
[7] Z. Yu, R. Guo and A.S. Bhalla: Mater. Lett. Vol. 57 (2002) p. 349.
[8] X.G. Tang, K.-H.Chew and H.L.W. Chan: Acta Mater. Vol. 52 (2004) p. 5177.
[9] Z. Yu, C. Ang, R. Guo and A.S. Bhalla: Mater. Lett. Vol. 61 (2007) p. 326.
[10] G.A. Smolensky, V.A. Isupov, A.I. Agranovskaya and N.N. Krainik: Sov. Phys. Solid State Vol. 2 (1962) p. 2651.
[11] C.F. Buhrer: J. Chem. Phys. Vol. 36 (1962) p. 798.
[12] J. Suchanicz, K. Roleder, A. Kania and J. Handerek: Ferroelectrics Vol. 77 (1988) p. 107.
[13] H. Nagata and T. Takenaka: J. Euro. Ceram. Soc. Vol. 21 (2001) p. 1299.
[14] H.-D. Li, C.-D. Feng and W.-L. Yao: Mater. Lett. Vol. 58 (2004) p. 1194.
[15] X.X. Wang, K.W. Kwok, X.G. Tang, H.L.W. Chan and C.L.Choy: Solid State Comm. Vol. 129, (2004) p. 319.
[16] R. Panton, C. Dubourdieu, F. Weiss, J. Kreisel, G. Köbernik and W. Haessler: Mater. Sci. Semicond. Process. Vol. 5 (2003) p. 237.

# ผลงานตีพิมพ์ในวารสารวิชาการระดับชาติ

*Journal of Metals, Materials and Minerals, Vol.20 No.3 pp.141-144, 2010*

# Synthesis of Lead–Free $Bi_{0.5}Na_{0.5}ZrO_3$ Powder

**Panupong JAIBAN, Sukanda JIANSIRISOMBOON and Anucha WATCHARAPASORN***

*Department of Physics and Materials Science, Faculty of Science,*
*Chiang Mai University, Chiang Mai 50200*

**Abstract**

In this study, an approach to synthesize bismuth sodium zirconate powders with the formula $Na_{0.5}Bi_{0.5}ZrO_3$ by mixed oxide method was investigated. The reaction involved mixtures of reagent grade $Bi_2O_3$, $Na_2CO_3$ and $ZrO_2$ powders. The mixtures were calcined at temperatures in the range of 700 - 850°C, and the starting composition was also subsequently changed by addition of $Bi_2O_3$, $Na_2CO_3$ or $ZrO_2$ powder at 5, 10 and 15 wt%. The calcined powders were analyzed using X-ray diffractometry. The result revealed that BNZ/$Na_2CO_3$ powders calcined at 800°C for 2 hours produced BNZ compound with maximum purity.

**Key words**: Lead-free ceramics, BNZ, Synthesis, Powder

## Introduction

In the past, many electrical devices such as multilayer capacitors (MLCCs), piezoelectric transducers, pyroelectric detectors/sensors, electrostrictive actuators, precision micropositioners, MEMs, etc. were all made from lead bearing compounds, e.g. lead titanate ($PbTiO_3$), lead zirconate titanate ($PbZr_{1-x}Ti_xO_3$), lead magnesium niobate ($Pb(Mg_{1/3}Nb_{2/3})O_3$), etc. However, volatilization of toxic PbO during high-temperature sintering causes environmental pollution.[4] Nowadays, several studies have attempted to find non-lead ceramics which may replace lead-based ceramics.[7] Examples are barium titanate ($BaTiO_3$), sodium niobate ($NaNbO_3$), bismuth potassium titanate ($Bi_{0.5}K_{0.5}TiO_3$) Nakata, *et al.*[5], bismuth litium titanate ($Bi_{0.5}Li_{0.5}TiO_3$), bismuth sodium titanate ($Bi_{0.5}Na_{0.5}TiO_3$), etc. Recently, bismuth sodium titanate (BNT) has received particular attention because of its interesting ferroelectricity at room temperature and high Curie temperature at 320°C. This solid solution was discovered by Smolenskii, *et al.*[8] and has been studied further by a number of researchers.[2-3, 6, 8] On the other hand, this material had drawbacks such as high coercive field ($E_c$ = 73 kV/cm) and high conductivity, resulting in the difficulty in poling process.[10] Many researchers also attempted to improve microstructure, mechanical properties, piezoelectric and electrical properties. Zirconium is one of many elements used as a modifier for the development of well-known $Pb(Zr_{1-x}Ti_x)O_3$ and $Ba(Zr_{1-x}Ti_x)O_3$ ceramics. Watcharapasorn, *et al.*[9] attempted to study this problem by investigating $Bi_{0.5}Na_{0.5}(Ti_{x-1}Zr_x)O_3$ with x = 0, 0.05, 0.1, 0.15 and 0.20. The result revealed that the density, grain size and hardness were increased with increasing Zr contents. The purpose of this study is to synthesize a new lead-free $Bi_{0.5}Na_{0.5}ZrO_3$ in which Ti was totally replaced by Zr and various conditions such as calcination temperature and starting compositions were varied to investigate their effect on compound formation.

## Materials and Experimental Procedures

$Bi_{0.5}Na_{0.5}ZrO_3$ (BNZ) powders were prepared by the conventional mixed oxide method. The starting chemicals used were $Bi_2O_3$ (99.9%, Aldrich), $Na_2CO_3$ (99.5-100.5%, RdH) and $ZrO_2$ (99%, Riedel-de Haën). The starting powders were weighed and ball milled in ethanol for 24 hours. The slurry was dried at 120°C for 24 hours. The mixed powders contained in alumina crucible were calcined at temperature ranging from 700 - 850°C for 2 hours. Then, the calcined powders were checked by X-ray diffraction method technique to find the appropriate temperature. After that, the starting composition which was subsequently changed by addition of $Bi_2O_3$, $Na_2CO_3$ or $ZrO_2$ powder at 5, 10 and 15 wt% was prepared by above process and then it was calcined at the appropriate temperature. Finally, the calcined powders were investigated once more by using an X-ray diffractometer and measurement of the amount of second phases was performed.

## Results and Discussion

After as-mixed $Bi_{0.5}Na_{0.5}ZrO_3$ (BNZ) powder was calcined at different temperatures, phase

*Corresponding author Tel: +66 5394 1921; Fax: +66 5394 3445; E-mail: anucha@stanfordalumni.org

formation was investigated by XRD as shown in Figure 1. From the results, it was found that the temperatures in range of 700°C - 750°C were not enough for completing the reaction. X-ray diffraction analysis showed that the sample contained a large amount of second phases. On the other hand, BNZ powders calcined at 850°C indicated that the materials began to partially react with alumina crucible and produced less pure BNZ powder. Therefore, based on this study, optimized calcination temperature was found to be 800°C. Figure 2 showed that the second phases appeared in range of $2\theta = 25 - 30$, 33, 46 and 50° which were most likely the phases of $Bi_2O_3$ and $ZrO_2$. However, $Na_2CO_3$ phase was not exhibited at temperature above 600°C.[1] It was expected therefore that addition of $Na_2CO_3$ should help complete the reaction. Hence, addition of 5, 10, 15 wt% $Na_2CO_3$ was carried out and the results are shown in X-ray patterns in Figure 3. The amount of second phases as indicated by a decrease in peak intensity in the region of $2\theta$ from 25-30° was clearly observed. Although both $Na_2CO_3$ and $Bi_2O_3$ have low melting point i.e. 850 and 820°C, respectively, the volatilization of $Na_2CO_3$ is not as well known as $Bi_2O_3$. In this study, it showed that $Na_2CO_3$ volatilized more than $Bi_2O_3$ and/or had dissociation problem at calcination temperature used. In order to check this hypothesis, $Bi_2O_3$ and $ZrO_2$ were also separately added into starting mixture. Figures 4 and 5 showed X-ray diffraction results of adding these two compounds, respectively. It showed that both $Bi_2O_3$ and $ZrO_2$ had nearly no effect on phase formation of $Bi_{0.5}Na_{0.5}ZrO_3$. This seemed to be in agreement with the existing second phases observed in Figure 2. The amount of second phases approximated from X-ray peak analysis of calcined powders with separately added $Na_2CO_3$, $Bi_2O_3$ and $ZrO_2$ are shown in Table 1. It was found that the relative concentration of impurity phase was ≈ 10.7 wt% in un-doped BNZ powder. Theses phases were decreased with increasing $Na_2CO_3$ content. However, at 15 wt% $Na_2CO_3$ content, it showed the second phase reduction was not significantly different from 10 wt% $Na_2CO_3$. For separate addition of $Bi_2O_3$ and $ZrO_2$ in BNZ powder, both can be seen that the amount of second phases clearly increased when compared with BNZ powder without their addition. Thus, from these results, reduction of second phases by using $Na_2CO_3$ additive could be confirmed. Hence, based on this study, the calcination temperature of 800°C and addition of excess $Na_2CO_3$ improved BNZ phase purity. Further improvement of phase purity by re-calcination and changing calcination time will be carried out and reported in the near future.

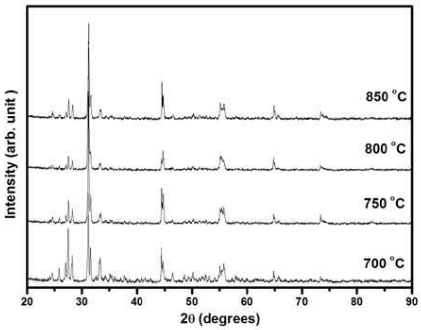


**Figure 1.** XRD patterns of BNZ powders calcined at different temperature for 2 hours.

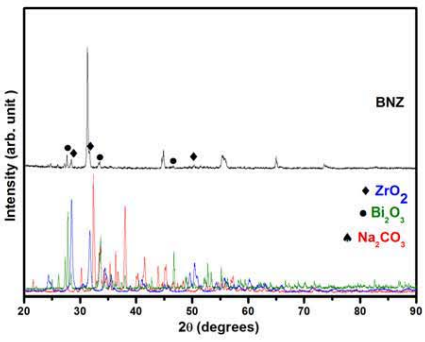


**Figure 2.** XRD pattern of BNZ powder calcined at 800°C for 2 hours compared with starting powder XRD pattern.

**Table 1.** amount of second phases of BNZ/$Na_2CO_3$, BNZ/$Bi_2O_3$ and BNZ/$ZrO_2$ powders.

| Amount of addition (%wt) | Second phases (%wt) of BNZ/$Na_2CO_3$ | Second phases (%wt) of BNZ/$Bi_2O_3$ | Second phases (%wt) of BNZ/$ZrO_2$ |
|---|---|---|---|
| 0 | 10.69 | 10.69 | 10.69 |
| 5 | 9.76 | 26.77 | 24.11 |
| 10 | 9.33 | 43.98 | 39.78 |
| 15 | 9.36 | 44.10 | 43.53 |

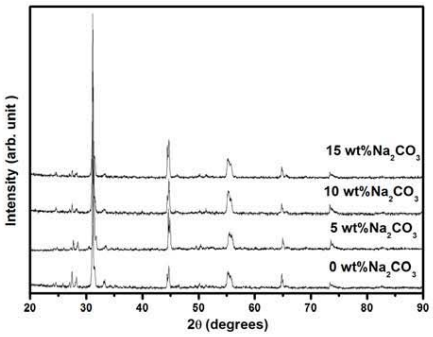


**Figure 3.** XRD patterns of $BNZ/Na_2CO_3$ powders calcined at 800°C for 2 hours.

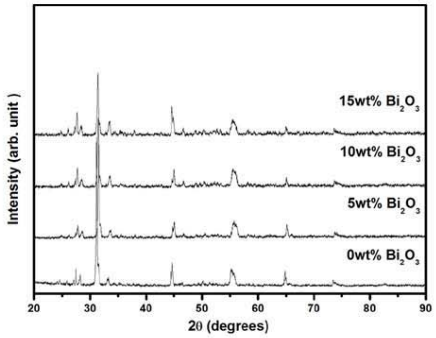


**Figure 4.** XRD patterns of $BNZ/Bi_2O_3$ powders calcined at 800°C for 2 hours.

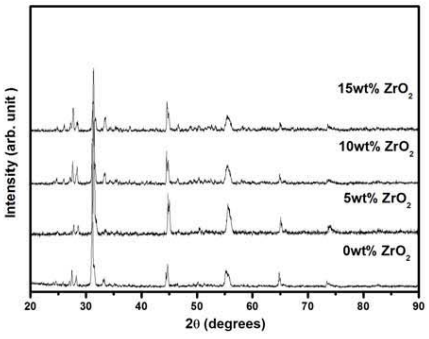


**Figure 5.** XRD patterns of $BNZ/ZrO_2$ powders calcined at 800°C for 2 hours.

## Conclusions

This research studied several factors affecting phase formation of new lead-free $Bi_{0.5}Na_{0.5}ZrO_3$ compound. Optimized conditions included calcination temperature of 800°C for 2 hours with addition of excess $Na_2CO_3$.

## Acknowledgments

This work is financially supported by the Thailand Research Fund, the National Research University Project under Thailand's Office of the Higher Education Commission, the Faculty of Science and the Graduate School, Chiang Mai University. P. Jaiban would also like to acknowledge financial support from the Thailand Research Fund through the Royal Golden Jubilee Ph.D. program.

## References

1. Bomlai, P., Wichianrat, P., Muensit, S. & Milne, S.J. (2007). Effect of calcination conditions and excess alkali carbonate on the phase formation and particle morphology of $Na_{0.5}K_{0.5}NbO_3$ powders. *J. Am. Ceram. Soc.* **90(5)** : 1650-1655.

2. Hagiyev, M.S., Ismailzade, I.H. & Abiyev, A.K. (1984). Pyroelectric properties of $(Na_{0.5}Bi_{0.5})TiO_3$ ceramics. *Ferroelectrics* **56(1)** : 215-217.

3. Isupov, V.A., Pronin, I.P. & Kruzina, T.V. (1984). Temperature dependence of birefringence and opalescence of the sodium-bismuth titanate crystals. *Ferroelectrics Letter* **2(6)** : 205-208.

4. Li, Y., Chen, W., Xu, Q., Zhou, J., Gu, X. & Fang, S. (2005). Electromechanical and dielectric properties of $Na_{0.5}Bi_{0.5}TiO_3$ – $K_{0.5}Bi_{0.5}TiO_3$ - $BaTiO_3$ lead-free ceramics. *Mater. Chem. Phys.* **94(2-3)** : 328-332.

5. Nagata, H., Yoshida, M., Makiuchi, Y. & Takenaka, T. (2003). Large piezoelectric constant and high curie temperature of lead-free piezoelectric ceramic ternary system based on bismuth sodium titanate-bismuth potassium titanate-barium titanate near the morphotropic phase boundary. *Jpn. J. Appl. Phys.* **42** : 7401-7403.

6. Pronin, I.P., Syrnikov, P.P., Isupov, V.A., Egorov, V.M. & Zaitseva, N.V. (1980). Peculiarities of phase transitions in sodium-bismuth titanate. *Ferroelectrics* **25(1)** : 395-397.
7. Rödel, J., Jo, W., Seifert, K.T.P., Anton, E.M., Granzow, T. & Damjanovic, D. (2009). Perspective on the development of lead-free piezoceramics. *J. Am. Ceram. Soc.* **92(6)** : 1153-1177.
8. Smolenskii, G.A., Isupov, V.A., Agranovskaya, A.I. & Krainik, N.N. (1961). New ferroelectrics of complex composition. *Sov. Phys. - Solid State* **2** : 2651–2654.
9. Watcharapasorn, A., Jiansirisomboon, S. & Tunkasiri, T. (2006). Microstructure and mechanical properties of zirconium-doped bismuth sodium titanate ceramics. *Chiang Mai J. Sci.* **33(2)** : 169.
10. Yuan, Y., Zhang, S. & Zhou, X. (2009). Effect of La occupation site on the dielectric and piezoelectric properties of $[Bi_{0.5}(Na_{0.75}K_{0.15}Li_{0.1})_{0.5}]TiO_3$ ceramics. *J. Mater. Sci.* – Mater. Electron. **20(11)** : 1090-1094.

*Journal of Microscopy Society of Thailand 2009, 23(1): 107-110*

# Microstructures and Mechanical Properties of Lead-Free Bismuth Sodium Titanate Zirconate Ceramics

Ampika Rachakom, Sukanda Jiansirisomboon, Anucha Watcharapasorn*
Department of Physics, Faculty of Science, Chiang Mai University, Chiang Mai, 50200, Thailand
*Corresponding author, e-mail: anucha@stanfordalumni.org

**Abstract**

Lead-free bismuth sodium titanate zirconate ceramics ($Bi_{0.5}Na_{0.5}Ti_{1-x}Zr_xO_3$ where x = 0.20, 0.35, 0.40, 0.45, 0.60 and 0.80) were fabricated using a conventional mixed-oxide method. All samples were calcined at temperatures ranging from 700-800 ºC for 2 h and sintered at a temperature of 900 ºC for 2 h. Higher sintering temperatures caused the ceramics, particularly those containing high Zr content, to melt and/or react with alumina crucible. The density of BNTZ ceramics was found to be in the range of 5.1-6.1 g/cm$^3$. Since the density values were found to increase with Zr concentration, it seemed that the ability to use low sintering temperature in this study was likely to be due to the lower melting point of ceramics with possible partial aid from very small amount of second liquid phase present as detected by X-ray diffraction analysis. SEM micrographs indicated a presence of small grains embedded between large grains especially in high Zr containing samples, causing a rather wide grain size distribution. Average grain size of BNTZ ceramics was found to range from 0.8 to 5.4 μm. In terms of mechanical properties, their dependence on Zr concentration was not obvious. Knoop hardness of BNTZ samples ranged from 2.8-4.8 GPa while Vickers showed the values of 3.2-5.4 GPa. Fracture toughness of these ceramics was found to be in the range of 1.1-2.9 MPam$^{1/2}$. These values were comparable to those of commercialized and widely investigated PZT and PLZT ceramics.

**Background**

It is well known that currently the PZT-based solid solutions have been widely used as actuators, transducers and sensors due to their excellent piezoelectric properties [1-3]. Currently, many other materials that possess high dielectric and piezoelectric coefficients still contain lead ions, for example, PMN-PT and PZN-PT [1-3]. Due to environmental concerns, many attempts to study non-lead systems with comparable electrical properties to those of lead-based ones have been carried out. Starting with $Ba(Ti,Zr)O_3$ solid solutions, several investigators have shown that these systems possessed broad dielectric contant-temperature curves indicating that addition of Zr into $BaTiO_3$ produced more diffused phase transition [4,5]. In addition, above 30 mol% Zr, the material showed relaxor behavior and these materials seemed to be suitable for tunable capacitors applications. The purpose of the present study is to investigate the microstructure and mechanical properties for bismuth sodium titanate zirconate ceramics fabricated by using conventional mixed-oxide method.

**Materials and Methods**

The $Bi_{0.5}Na_{0.5}Ti_{1-x}Zr_xO_3$ ceramics with x = 0.20, 0.35, 0.40, 0.45, 0.60 and 0.80 were prepared by mixed oxide method powders. The starting powders of $Bi_2O_3$ (>98%, Fluka), $Na_2CO_3$ (99.5%, Carlo Erba), $TiO_2$ (>99%, Riedel de Haën) and $ZrO_2$ (>99%, Riedel de Haën) were mixed in ethanol using zirconia ball milling media. After drying, the calcination was carried out at 800 ºC/2h for composition x = 0.20, 0.35, 0.40 and 0.45, and at 700 ºC/2 h for composition x = 0.60 and 0.80. The calcined powders were then ball milled again for 6 h. Phase development and crystallographic structure of the powders were examined by X-ray diffraction. The calcined powders were uniaxially pressed into the pellets before being sintered at 900 ºC for 2 hours and re-checked for phase purity using X-ray diffraction technique. For microstructural investigation, the ceramics were polished and thermally etched at 800ºC for 15 minutes.

The density and microstructure of ceramics were evaluated by Archimedes method and scanning electron microscopy (SEM), respectively. The theoretical density was approximated from the unit cell size and its constituent ions with an assumption that the lattice type remained the same and only the lattice parameter changed with composition. The grain size was determined from the SEM micrograph using mean linear interception. The well-polished ceramics were subjected to Knoop (Matsuzawa MXT-α) and Vickers (Galileo Microscan 2) indentations for hardness (i.e. $H_v$ and $H_k$) measurements. Young's modulus ($E$) and fracture toughness ($K_{IC}$) were determined following method described by Antais et al. [5] and Marshall et al. [6]. SEM images of indented areas were employed to determine all of these mechanical properties.

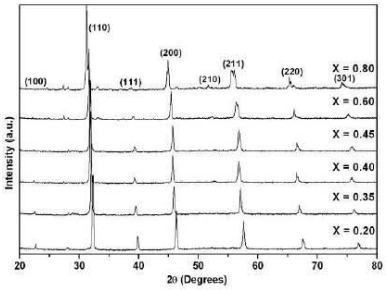


**Fig.1** XRD pattern of $Bi_{0.5}Na_{0.5}Ti_{1-x}Zr_xO_3$ ceramics.

## Results and Discussion

X-ray diffraction pattern of $Bi_{0.5}Na_{0.5}Ti_{1-x}Zr_xO_3$ (where x = 0.20, 0.35, 0.40, 0.45, 0.60 and 0.80) ceramics were show in Fig. 1. It can be seen the peaks of $Bi_{0.5}Na_{0.5}Ti_{0.8}Zr_{0.2}O_3$ systematically shifted to the left. This indicated that the unit cell expanded. This is in agreement with th e fact that the ionic size of Zr ion ($r_{Zr4+}$ = 0.72 Å) is larger than the ionic size of Ti ion ($r_{Ti4+}$= 0.61 Å). Based on the relative intensities of X-ray diffractions peaks, one of the apparent feature observed was the reduction in peak intensity of (100) and (111) reflections.

From preliminary investigation of crystal structure change due to the replacement of Zr in Ti lattices, it was found that the reduction of these reflections came from the differences in scattering factor and ionic size of Zr compared to those of Ti when the rhombohedral lattice was kept the same. This suggested that the lattice was distorted such that the reflecting planes of atoms for these reflections caused higher degree of destructive interference with increasing Zr concentration. Another observable feature was the splitting of X-ray peaks especially in the sample with x = 0.60 and 0.80. From crystal structure investigation, if the unit cell expanded while maintaining the rhombohedral structure, this peak splitting seemed to be naturally occurred. Small amount of second phases was also present in the samples which could possibly be bismuth oxide or some Zr-rich phase based on SEM-EDS results. However, these second phase were not expected to have significant effects on mechanical properties of BNTZ ceramics.

The microstructures of the BNTZ ceramics are illustrated in Fig. 2. The density of sample with x = 0.2 was relatively low compared to those containing higher Zr content. The density for most samples was found to be in the range of 5.9-6.1 g/cm$^3$ which corresponded to the relative density of at least 95% of their theoretical values. The average grain size was found to range from 0.8-5.4 μm. Although it seemed that the grain size increased with Zr content but the change was only observed in low-Zr sample. In high-Zr sample, nearly no change in grain size was observed but there was smaller grains along the grain boundaries of the matrix grains which could be part of the grain growth inhibition in high Zr sample. These smaller grains were found to be Zr-rich phase as determined from SEM-EDS technique.

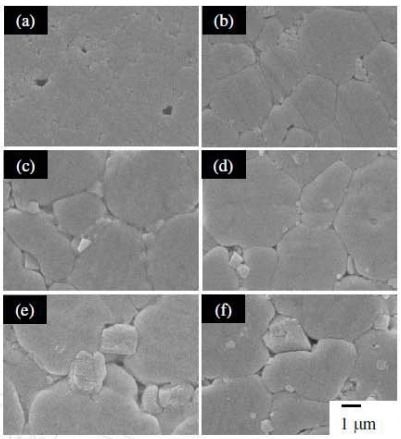


**Fig.2** SEM micrograph of $Bi_{0.5}Na_{0.5}Ti_{1-x}Zr_xO_3$ ceramics, where x = (a) 0.20, (b) 0.35, (c) 0.40, (d) 0.45, (e) 0.60 and (f) 0.80

Figure 3 shows backscattered electron images of representative BNTZ ceramic samples along with their corresponding EDS spectrum. It could be observed that relative intensity of Zr peaks were different between these two samples indicating the different amount of Zr present in the matrix phase. Despite the fact that there are some uncertainties associated with quantitative analysis using this technique, the EDS spectrum still gave higher concentration of Zr for $Bi_{0.5}Na_{0.5}Ti_{0.2}Zr_{0.8}O_3$ sample than the one containing lower Zr content. This higher amount of substitution corresponded well to the shift in X-ray peaks.

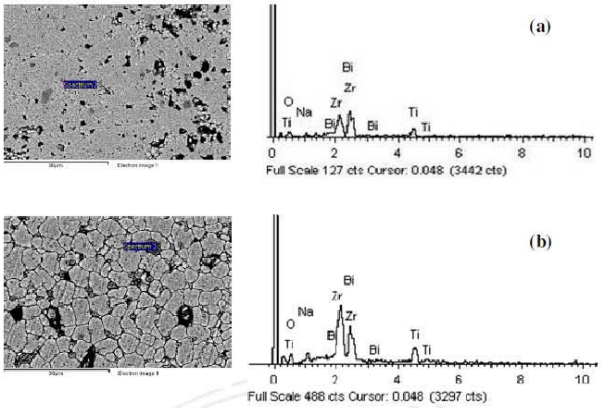


**Fig.3** Backscattered electron images and EDS spectra of $Bi_{0.5}Na_{0.5}Ti_{1-x}Zr_xO_3$ ceramics: (a) x = 0.2 and (b) x = 0.8.

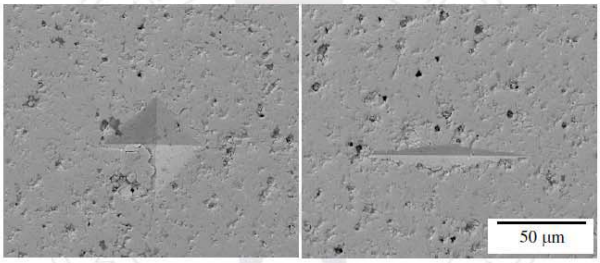


**Fig.4** SEM micrograph of $Bi_{0.5}Na_{0.5}Ti_{1-x}Zr_xO_3$ where x=0.40, showing (a) Vickers and (b) Knoops indentation impressions.

**Table 1** Physical and mechanical property of BNTZ ceramics

| $Bi_{0.5}Na_{0.5}Ti_{1-x}Zr_xO_3$ | Density (g/cm$^3$) | Grain size (µm) | Mechanical property | | | |
|---|---|---|---|---|---|---|
| | | | $H_K$ | $H_V$ | E(GPa) | $K_{IC}$ (MPa m$^{1/2}$) |
| 0.20 | 5.1 | 0.78 ± 0.10 | 4.45 ± 0.49 | 4.33 ± 0.32 | 60 | 1.25 |
| 0.35 | 6.0 | 2.63 ± 0.17 | 3.63 ± 0.14 | 3.97 ± 0.26 | 89 | 1.34 |
| 0.40 | 5.9 | 5.37 ± 0.47 | 4.76 ± 0.62 | 5.24 ± 0.47 | 143 | 2.86 |
| 0.45 | 5.9 | 4.18 ± 0.29 | 2.78 ± 0.78 | 3.24 ± 0.50 | 63 | 1.06 |
| 0.60 | 6.0 | 4.77 ± 0.52 | 4.26 ± 0.10 | 5.44 ± 0.24 | 140 | 1.95 |
| 0.80 | 6.1 | 4.63 ± 0.38 | 3.17 ± 0.76 | 4.09 ± 0.16 | 110 | 1.49 |

Mechanical properties of the ceramics in terms of Knoop hardness ($H_K$), Vickers hardness ($H_V$), Young's modulus ($E$) and fracture toughness ($K_{IC}$) were investigated and their values are listed in Table 1. The hardness value dependence on Zr concentration was not obvious. The Knoop hardness was found to range from 2.8-4.8 GPa, while Vickers hardness was 3.2-5.4 GPa. The Young's modulus and fracture toughness were found to be about 60-140 GPa and 1.1-2.9 MPam$^{1/2}$, respectively. Therefore, compared to the values obtained for the widely investigated PZT and PLZT ceramics which had the hardness and fracture toughness of about 3-5 GPa and 1.0-1.5 MPam$^{1/2}$ [1], the BNTZ ceramics seemed to possess good mechanical properties suitable for actuator applications.

Figure 4 shows Vickers and Knoop hardness indentation impressions of a BNTZ ceramic. Compared to the grain size, the indented area was much larger and therefore the variation in mechanical properties of the samples could be largely due to microstructural inhomogeneities. Further studies will be needed to separate the effect of grain boundaries from the grains themselves.

**Conclusion**

Lead-free $Bi_{0.5}Na_{0.5}Ti_{1-x}Zr_xO_3$ ceramics (where x = 0.20, 0.35, 0.40, 0.45, 0.60 and 0.80) were successfully fabricated. X-ray diffraction patterns showed a systematic shift to the left, indicating the expansion of unit cell when Zr concentration increased in agreement with ionic size consideration. All ceramic samples showed dense microstructure with grain size variation dependence on Zr content. The mechanical properties of BNTZ ceramics did not show significant dependence on composition. Nevertheless, their values especially the hardness and fracture toughness were found to be comparable to those of PZT and PLZT which suggested that these materials may be suitable for actuator applications.

**Acknowledgements**

This research is financially supported by the Thailand Research Fund (TRF) and the Commission on Higher Education (CHE). Authors would also like to thank the Graduate School and the Faculty of Science, Chiang Mai University.

**References**

1. Uchino K. **Piezoelectric Actuators and Ultrasonic Motors**, *Boston, Kluwer Academic* 1997.
2. Moulson AJ, Herbert JM. **Electroceramics, 2nd Ed.**, *West Sussex, Wiley* 2003.
3. Haertling GH. Ferroelectric Ceramics: History and Technology. *J. Am. Ceram. Soc*. 1999, 82: 797-818.
4. Yu Z, Ang C, Guo R, Bhalla AS. Dielectric properties of $Ba(Ti_{1-x}Zr_x)O_3$ solid solutions. *Mater. Lett*. 2007, 61: 326–329.
5. Tang XG, Chew KH, Chan HLW. Diffuse phase transition and dielectric tunability of $Ba(Zr_yTi_{1-y})O_3$ relaxor ferroelectric ceramics, *Acta Mater*. 2004, 52: 5177–5183.
6. Antis GR, Chantikul P, Lawn BR, Marshall DB. A critical evaluation of indentation technigues for measuring fracture toughness. *J. Am. Ceram. Soc.* 1981, 64: 533-538.
7. Marshall DB, Noma T, Evans AG. A simple method for determining elastic modulus-to-hardness ratio using Knoop indentation measurement. *J. Am. Ceram. Soc.* 1982, 65: C175-176.

การนำเสนอผลงานในการประชุมวิชาการนานาชาติ

ISEPD 2011

www.isepd.org

# ISEPD2011

## The 12th International Symposium on Eco-Materials Processing and Design

January 8-11, 2011

The Empress Hotel Chiang Mai, Thailand

Proceedings

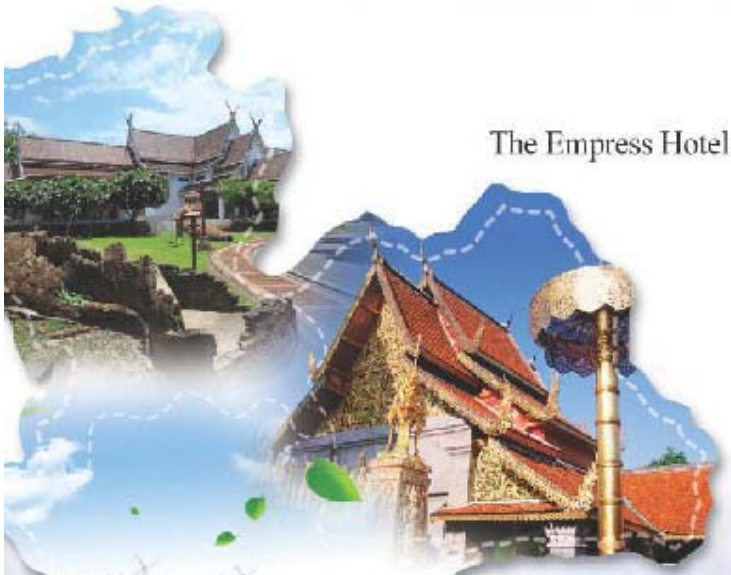

**Organized by**

Faculty of Science, Chiang Mai University, Thailand

Sun Moon University, Korea

**Sponsored by**

AOARD Foresight Program by JSPS, NSFC, NRF

US Army

US Airforce

Thailand's Office of the Higher Education Commission through the National Research University Project

Materials Science Research Center, Faculty of Science, Chiang Mai University

Nanoscience and Nanotechnology Research Center, Faculty of Science, Chiang Mai University

U.S. ARMY RDECOM

Poly(ethersulfone)s carrying pendant sulfonated imide side group. The first step in the preparation involved nitration of poly(ethersulfone) (ultrason®-S6010), with ammonium nitrate and trifluoroacetic anhydride resulting in the nitrated poly(ethersulfone) (NO2-PES). In the second step, the nitro groups on polymer were reacted with tin(II)chloride and sodium iodide as reducing agents for creating the amino poly(ethersulfone) (NH2-PES). The imide-poly(ethersulfone)s (IPES) were obtained by reaction of phthalic anhydride and the amino-poly(ethersulfone) with triethyl amine. The sulfonated imide-poly(ethersulfone)s (SIPES) were prepared by chlorosulfonic acid. The different degrees of sulfonated imide units of poly(ethersulfone) were successfully synthesized by an optimized condition. The Sulfonated imide-poly(ethersulfone)s (SIPES) were studied by FT-IR, 1H-NMR spectroscopy and thermo gravimetric analysis (TGA). Sorption experiments were conducted to observe the interaction of sulfonated polymers with water. The ion exchange capacity (IEC) and proton conductivity of SIPES membranes were evaluated with increase of degree of sulfonation. The water uptake of synthesized SIPES membranes exhibit 30～65% compared with 28% of Nafion 211®. The SIPES membranes exhibit proton conductivities (25°C) of 1.21-2.62×10-3 S/cm compared with 3.37×10-3 S/cm of Nafion 211®.

**Keywords:** Polyimide, Poly(ethersulfone), Membrane, PEMFC, Proton exchange membrane, Proton conductivity

**P - A 37**

### *Preparation of Bismuth Sodium Zirconate Powder by Mixed Oxide Method*

Panupong Jaiban, Ampika Rachakom, Napatporn Petnoi, Suwapitcha Buntham, Sukanda Jiansirisomboon, Anucha Watcharapasorn

Department of Physics and Materials Science, Faculty of Science, Chiang Mai University, Chiang Mai 50200, Thailand

Lead-free bismuth sodium zirconate powder with formula Na0.5Bi0.5ZrO3 was prepared by conventional mixed oxide method. Bismuth sodium zirconate (BNZ) powder with 10 wt% Na2CO3 was calcined at 800°C for 2 h dwell time. Investigation of the effects of re-calcination and dwell time on phase formation of powders was also carried out. The results revealed that re-calcinaton significantly affected the formation of single-phase BNZ powder. Phase characteristics were checked by X-ray diffraction (XRD). Powder cell software was employed to simulate crystal structure of BNZ powder. It was found that BNZ powder most likely possessed an orthorhombic structure. Microstructure and chemical composition were characterized by scanning electron microscopy (SEM) and energy-dispersive (EDX) techniques, respectively. Thermo-gravimetric analyzer (TGA) and differential scanning calorimetry (DSC) were used to study thermal transformation of starting compound. Relationships between these properties and phase formation were discussed in details.

**Keywords:** BNZ powder, Crystal structure, Lead-free powder, Preparation, Mixed oxide method

**P - A 38**

### *Preparation, Electrochemical Properties and Cytotoxicity Assessment of Nanosized CuO/La2O3/CeO2 Composite for the Decomposition of Gaseous Ammonia*

Chang-Mao Hung

Department of Vehicle Engineering, Yung-Ta Institute of Technology and Commerce, Taiwan

This work considers the CuO/La2O3/CeO2 nano-rare earth composite materials were synthesized by coprecipitation method with aqueous solutions of copper nitrate, lanthanum nitrate and cerium nitrate. The performance of the selective catalytic oxidation of ammonia to N2 (NH3-SCO) over a CuO/La2O3/CeO2 nano-rare earth composite materials in a tubular fixed-bed reactor (TFBR) at temperatures from 423 to 673 K in the presence of oxygen was reported. The catalytic redox behaviors were determined by cyclic voltammetry (CV). Further, cell cytotoxicity and the percentage cell survival were determined by using MTS assay on human fetal lung tissue cell (MRC-5). The experimental results show that the

**Keywords:** Solar cells, III-V heterostructures, Fianite, YSZ, Antireflection coating

**P - A 27**

### *Influence of Ramp Time of Close Spaced Sublimation on Crystal Structure, Optical and Electrical Properties of CdTe Thin Films*

Thitinai Gaewdang, Ngamnit Wongcharoen, Waraporn Bunkua, Chanya Thaisatuen
School of Physics, Faculty of Science, King Mongkut's Institute of Technology Ladkrabang

CdTe thin films were deposited by close-spaced sublimation(CSS) method on glass substrate in vacuum at a pressure of $3.0\times10^{-2}$mbar. The samples were prepared under four ramp time conditions: 20, 30, 40 and 50 minutes. During this work, the temperature of the precursor and the substrate were fixed at 550 and 450°C respectively. Crystal structure of these films were checked by X-ray diffraction method. CdTe thin films are polycrystalline belonging to cubic structure with a preferential orientation of (111) plane.The grain size and surface morphology of the films was studied by using Scanning Electron Microsope (SEM). The biggest grain size about 8.16 $\mu$m were observed at ramp time 40 min. The optical transmission spectrum of CdTe thin films were performed by UV-Vis spectrophotometer with wavelength in the range 600～1,000 nm. Thus, energy gap value of each ramp time was obtained from the spectral transmission data. The electrical properties of CdTe thin films were performed by using dark current-voltage and light current-voltage measurements. The resistivity of the films around $1\times10^{6}$ $\Omega$•cm was observed at room temperature. Resistivity values of all samples decrease under illumination by ELH halogen lamp.

**Keywords:** CdTe thin films, Close-spaced sublimation, XRD

**P - A 28**

### *Investigation of Morphotropic Phase Boundary for Bi0.5Na0.5Ti1-xZrxO3 Solid Solutions by X-ray Diffraction Technique*

Ampika Rachakom, Anucha Watcharapasorn, Panupong Jaiban, Napatporn Petnoi, Sukanda Jiansirisomboon
Physics and Materials Faculty of Science, Thailand

Binary solid solutions system of lead-free bismuth sodium titanate zirconate (Bi0.5Na0.5ZrxTi1-xO3 or BNTZ) powders were prepared by a conventional mixed-oxide method with varied composition of x = 0.40, 0.45, 0.50, 0.55, 0.60 and 0.65 mole fraction. Preliminary X-ray diffraction analysis of BNTZ at low Zr ($x<0.40$) showed the unit cell expansion while maintaining rhombohedral structure. At high Zr ($x>0.60$) however, peak splitting occurred and this seemed to indicate a distorted tetragonal or orthorhombic structure. Thus, this study intended to investigation the existence of morphotropic phase boundary (MPB) using the change in crystal structure and graphical analysis based on X-ray diffraction patterns.

**Keywords:** BNT, BNZ, Morphotropic phase boundary, X-ray diffraction

**P - A 29**

### *Kinetic Study of CdS Thin Films Prepared by Chemical Bath Deposition Method and Their Characteristics for Solar Cell Applications*

Ju-Young Park[1], Ki Hoon Kim[1], Kyu-Jung Cho[2], Chaehwan Jeong[2]
[1]CeNSCMR, Department of Physics and Astronomy, Seoul National Univisity, Seoul 151-747, [2]Solar Cell Research Group,

www.amf-amec-2010.org

# The 7th AMF-AMEC-2010

## The 7th Asian Meeting on Ferroelectricity and the 7th Asian Meeting on ElectroCeramics

June 28 - July 1, 2010
Ramada Plaza Jeju Hotel, Jeju, Korea

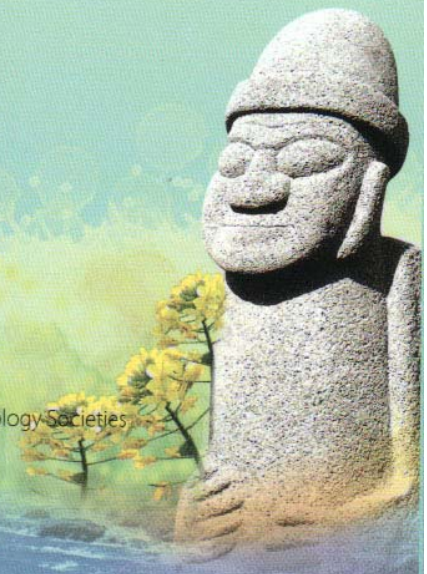

**Organized by**
The Korean Physical Society
The Korean Ceramic Society

**Sponsored by**
Korean Federation of Science and Technology Societies
National Research Foundation of Korea
IEEE-UFFC
Lotte Scholarship Foundation
Hynix Semiconductor Inc
Nextron Corporation
Park Systems
Seoul National University
BK 21 Materials Education and Research Division, Seoul National University
Kyonggi University
The Basic Science Research Institute, University of Ulsan
The Institute for Basic Science, Changwon National University
Jeju Special Self-Governing Province
Korea Tourism Organization

**2-e-P03**

## Synthesis and Characterization of Bismuth Sodium Zirconate Powders

**P. Jaiban*, S. Jiansirisomboon and A. Watcharapasorn+**
Department of Physics and Materials Science, Chiang Mai University, Chiang Mai 50200, Thailand

*E-mail of the first author: panupong_jaiban@hotmail.com
+E-mail of the corresponding author: anucha@stanfordalumni.org

In this study, an approach to synthesize bismuth sodium zirconate powders with a formula $Na_{0.5}Bi_{0.5}ZrO_3$ by mixed oxide method was investigated. Bismuth sodium zirconate (BNZ) powders were characterized by X – ray diffraction (XRD), scanning electron microscopy (SEM) and energy – dispersive X – ray (EDX) techniques. The effect of calcination temperature and dwell time on phase formation of the powders was examined. It was found that the calcination temperature and dwell time had a pronounced effect on phase formation of the calcined BNZ powders. Optimization of calcination conditions could produce single-phase $Na_{0.5}Bi_{0.5}ZrO_3$ having most likely a distorted tetragonal structure. Rietveld analysis was employed to characterize the exact crystal structure and its relationship to ferroelectric and piezoelectric properties.

The 7th AMF-AMEC-2010
7th Asian Meeting on Ferroelectricity and 7th Asian Meeting on ElectroCeramics
JEJU-Korea

**2-e-P02**

# Preparation and Phase Transformation of $Bi_{0.5}Na_{0.5}Zr_xTi_{1-x}O_3$

**A. Rachakom*, S. Jiansirisomboon, and A. Watcharapasorn+**
Department of Physics and Materials Science Faculty of Science Chiang Mai University, Chiang Mai, 50200, Thailand

*E-mail of the first author: a.rachakom@hotmail.com
+E-mail of the corresponding author: anucha@stanfordalumni.org

In this research, lead-free bismuth sodium titanate zirconate ($Bi_{0.5}Na_{0.5}Zr_xTi_{1-x}O_3$ or BNTZ) powders (x = 0.20, 0.35, 0.40, 0.45, 0.60 and 0.80 mole fraction) were prepared by a conventional mixed-oxide method by varying factor of time, temperature calcinations and excess $Na_2CO_3$. Preliminary, X-ray diffraction analysis showed a systematic peak shift in the pattern indicating that the unit cell size increased with increasing Zr content. From crystal structure investigation, at low Zr concentration the unit cell expanded while maintaining rhombohedral structure. At high Zr concentration, however, peak splitting occurred and this seemed to indicate a distorted tetragonal structure. Thus, author was studied Quantitative analysis using Rietveld refinement analysis on X-ray diffraction pattern data of BNTZ powder were carried out in order to relate the crystallographic information to their ferroelectric and piezoelectric properties.

การนำเสนอผลงานในการประชุมวิชาการระดับชาติ

Proceedings of the

# MST28 2011

# ANNUAL CONFERRENCE

The 28th Annual Conferrence

of the Microscopy Society of Thailand

January 5-7, 2011

Mae Fah Luang University,

Chiang Rai,Thailand

Organized by

Poster Presentation

# Effects of Sintering Temperatures on Preparation of BNZ Ceramic

P. Jaiban[1], A. Rachakom[1], P. Petnoi[1], S. Jiansirisomboon[1] and A. Watcharapasorn [1*]
[1]Department of Physics and Materials Science, Faculty of Science, Chiang Mai University, Chiang Mai, Thailand
*Corresponding author, e-mail: anucha@stanfordalumni.org

**Abstract**

In this research, effects of sintering temperatures on preparation of lead-free bismuth sodium zirconate ceramic were investigated. BNZ powder with 10 wt% $Na_2CO_3$ was prepared by mixed oxide method. Phase characteristic of calcined powder was checked by X-ray diffraction technique. It was found that BNZ powder has an orthorhombically distorted perovskite ($ABO_3$) structure. Then, BNZ ceramics were fabricated by solid-state sintering and were sintered in a temperature range of 900 – 1100 $^{O}$C for 2 h. From the results, BNZ ceramic sintered at 1050 $^{O}$C showed maximum relative density. XRD patterns indicated that complete solid solution ceramic appeared at 900 and 950 $^{O}$C. Non-perovskite phase existing in BNZ ceramics was found to be $ZrO_2$. Scanning electron microscopy was used to study microstructure. It could be seen that grain growth of all BNZ ceramics increased with increasing sintering temperatures. However, evaporations of bismuth or sodium based composition seemed to affect grain growth and induced porosity in this system. Relationship between competing mechanism of evaporation and densification of BNZ ceramic were discussed in details.

PM

**References**

1. J. Rödel, W. J. Klaus, T. P. Seifert, E. M. Anton, T. Granzow, Perspective on the development of lead-free piezoceramics, J. Am. Ceram. Soc. 92, 1153-1177 (2009).
2. X. H. Wang, R. Z. Chen, Z. Gui, T. L. Long, The grain size effect on dielectric properties of $BaTiO_3$ based ceramics, Mats. Sci. Eng. 99, 199-202 (2003).
3. X. Chou, J. Zhai, X. Yao, Relaxor behavior and dielectric properties of $La_2O_3$ doped barium zirconate titanate ceramics for tunable device applications, Mats. Chem. Phys. 109, 125-130 (2008).
4. G. A. Smolenskii, V. A. Isupov, A. I. Agranovskaya, N. N. Krainik, New ferroelectrics of complex composition, Sov. Phys. Solid. State. 2, 2651-2654 (1961).
5. H. Nagata, T. Takenaka, Additive effects on electrical properties of $Bi_{1/2}Na_{1/2}TiO_3$ ferroelectric ceramics, J. Eur. Ceram. Soc. 21, 1299-1302 (2001).
6. Y. Yamada, T. Akutsu, H. Asada, K. Nozawa, S. Hachiga, T. Kurosaki, O. Ikagawa, H. Fujiki, K. Hozumi, T. Kawamura, T .Amakawa, K. I. Hirota, T. Ikeda, Effect of B-ions substitution in $[(K_{1/2}Bi_{1/2})$-$(Na_{1/2}Bi_{1/2})](Ti\text{-}B)O_3$ system with B = Zr, $Fe_{1/2}Nb_{1/3}$, $Zn_{1/3}Nb_{2/3}$ or $Mg_{1/3}Nb_{2/3}$, Jpn. J. Appl. Phys. 34, 5462-5466 (1995).

Poster Presentation

# Characteristics of Nb doped $Bi_{0.5}Na_{0.5}Ti_{0.41}Zr_{0.59}O_3$ Ceramics

Ampika Rachakom, Panupong Jaiban, Sukanda Jiansirisomboon, Anucha Watcharapasorn*
Department of Physics and Materials science, Faculty of Science, Chiang Mai University, Chiang Mai, 50200, Thailand
*Corresponding author, e-mail: anucha@stanfordalumni.org

**Abstract**

Lead-free Nb doped Bismuth Sodium Titanate Zirconate ($Bi_{0.5}Na_{0.5}Ti0_{.41}Zr_{0.59}O_3$, BNTZ) ceramics with [illegible] = 0, 0.01, 0.03, 0.05, 0 07 and 0.009 mole fraction was synthesized by the conventional mixed oxide method. All samples were calcined at 700 $^0$C for 2h, pressed into the pellet and sintered at 900$^0$C for 2h. The Nb-doped BNTZ ceramics were characterized using X–ray diffraction (XRD) and scanning electron microscope (SEM). The results showed that the crystal structure was rhombohedral phase. The SEM micrographs indicated that average grain sizes tended to decrease with increasing Nb concentration while the relative density values were at least 95% of theoretical value. In addition, the phases found in these ceramics were also identified using energy dispersive X-ray analysis (EDX).These information will be correlate to their measured properties.

**References**

1. B. Jaffe, W.R. Cook, H. Jaffe, Piezoelectric ceramics, Academic press, London, UK, (1971).
2. G.H. Haertling, Ferroelectric ceramics: history and technology, J. Am. Ceram. Soc. 82(4), 797-818 (1999).
3. A.J. Moulson, J.M. Herbert, Electroceramics: materials, properties, applications, John Wiley & Sons, Chichester (2003).
4. C.-L. Huang, B.-H. Chen, L. Wu, Variability of impurity doping the modified Pb(Zr, Ti)O3 ceramics of type ABO3, Solid State Commun. 130, 19-23(2004).
5. M. Pereira, A.G. Peixoto, M.J.M. Gomes, Effect of Nb doping on the microstructure and electrical properties of the PZT ceramics, J. Euro. Ceram. 21, 1353-1356(2001).
6. S.-Y. Chu, T.Y. Chen, I-T. Tsai, W. Water, Doping effects of Nb additives on the piezoelectric and dielectric properties of PZT ceramics and its application on SAW device. Sensor Actuat. A-Phys. 113, 198-203(2004).
7. Y. Yamada, T. Akutsu, H. Asada, K. Nozawa, S. Hachiga, T. Kurosaki, O. Ikagawa, H. Fujita, H. Hozumi, T. Kawamura, T. Amakawa, K.-I. Hirota, T. Ikeda, Effect of B-ion substitution on [(K1/2Bi1/2)-(Na1/2Bi1/2)] (Ti-B)O3 system with B = Zr, Fe1/2, Nb1/2, Zn1/3Nb2/3 or Mg1/3Nb2/3, Jpn. J. Appl. Phys. 34 , 5462-5466(1995).
8. Md. A. Mohiddon, R. Kumar, P. Geol , K.L. Yadav, Effect of Nb doping on structural and electrical properties of PZT (65/35) ceramics. IEEE. T. Dilectric. In. 14(2007) 204-211.

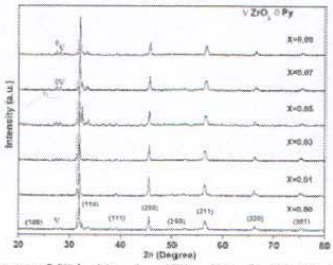


**Figure 1** X-ray diffraction patterns of $[Bi_{0.5}Na_{0.5}]_{1-x/2}[Ti_{0.41}Zr_{0.59}]_{1-x}Nb_xO_3$ ceramics when x= 0, [illegible], 0.05, 0.07 and 0.09, respectively.

6th MSAT

PROCEEDINGS

# The Sixth Thailand Materials Science and Technology Conference

*In conjunction with*

**The Sixth National Chitin - Chitosan Conference**

**Thailand Textile Symposium 2010**

*August 26-27, 2010*

*Miracle Grand Convention Hotel, Bangkok, Thailand*

Organized by

MTEC a member of NSTDA

สวทช NSTDA

Conference Sponsors

Western Digital · COTTO · ptt CHEM · SAMMITR · Delcam · crest · PCL HOLDING Co.,LTD บริษัท พี ซี แอล ไฮลดิ้ง จำกัด · ENTECH · ELSEVIER · LMS

# Synthesis of Lead–free $Bi_{0.5}Na_{0.5}ZrO_3$ Powder

**Panupong Jaiban**, Sukanda Jiansirisomboon and Anucha Watcharapasorn*
Department of Physics and Materials science, Faculty of Science, Chiang Mai University, Chiang Mai 50200
*Corresponding Author: Tel. (053) 941921, Fax. (053) 943445, E-mail: anucha@stanfordalumni.org

**Abstract**

In this study, an approach to synthesize bismuth sodium zirconate powders with a formula $Na_{0.5}Bi_{0.5}ZrO_3$ by mixed oxide method was investigated. The reaction involved mixtures of reagent grade $Bi_2O_3$, $Na_2CO_3$ and $ZrO_2$ powders. The mixtures were calcined at temperature in the range of 700 - 850 °C and the starting composition was also subsequently changed by addition of $Bi_2O_3$, $Na_2CO_3$ or $ZrO_2$ powder at 5, 10 and 15 wt%. The calcined powders were analyzed using X-ray diffractrometry. The result revealed that BNZ/$Na_2CO_3$ powders calcined at 800 °C for 2 h produced BNZ compound with maximum purity.

***Keywords**: Lead-free ceramics; BNZ; Synthesis; Powder*

## 1. Introduction

In the past, many electrical applications such as multilayer capacitors (MLCCs), piezoelectric transducers, pyroelectric detectors/sensors, electrostrictive actuators, precision micropositioners, MEMs, etc. were all lead bearing compounds, e.g. lead titanate ($PbTiO_3$), lead zirconate titanate ($PbZr_{1-x}Ti_xO_3$), lead magnesium niobate ($PbMg_{1/3}Nb_{2/3}O_3$), etc. However, volatilization of toxic PbO during high-temperature sintering causes environmental pollution [1]. Nowadays, several studies attempted to find non-lead ceramics which could replace lead-based ceramics. Examples were barium titanate ($BaTiO_3$), sodium niobate ($NaNbO_3$), bismuth potassium titanate ($Bi_{0.5}K_{0.5}TiO_3$) [2], bismuth litium titanate ($Bi_{0.5}Li_{0.5}TiO_3$), bismuth sodium titanate ($Bi_{0.5}Na_{0.5}TiO_3$), etc. Recently, bismuth sodium titanate (BNT) has been widely studied because of its interesting ferroelectricity at room temperature and high Curie temperature at 320 °C. This solid solution was discovered by Smolenskii *et al*. [3] and has been studied further by a number of researchers [3-6]. On the other hand, this material had drawbacks of high coercive field ($E_c$ = 73 kV/cm) and high conductivity, resulting in the difficulty in poling process [7]. Many researchers attempted to improve microstructure, mechanical properties, piezoelectric and electrical properties. Zirconium is one of many elements used as a modifier for the development of well-known $Pb(Zr_{1-x}Ti_x)O_3$ and $Ba(Zr_{1-x}Ti_x)O_3$ ceramics. Watcharapasorn *et al*. [8] attempted to study this problem by investigating $Bi_{0.5}Na_{0.5}(Ti_{x-1}Zr_x)O_3$ with x = 0, 0.05, 0.1, 0.15 and 0.20. The result revealed that the density, grain size and hardness were increased with increasing Zr contents. The purpose of this study is to synthesize a new lead-free $Bi_{0.5}Na_{0.5}ZrO_3$ in which Ti was totally replaced by Zr and various conditions such as calcination temperature and starting compositions were varied to investigate their effect on compound formation.

## 2. Experimental procedures and methods

$Bi_{0.5}Na_{0.5}ZrO_3$ (BNZ) powders were prepared by the conventional mixed oxide method. The starting chemicals used were $Bi_2O_3$ (99.9%, Aldrich), $Na_2CO_3$ (99.5-100.5%, RdH) and $ZrO_2$ (99%, Riedel-de Haën). The starting powders were weighed and ball milled in ethanol for 24 h. The slurry was dried at 120 °C for 24 h. The mixed powders contained in alumina crucible were calcined at temperature ranging from 700 - 850 °C for 2

h. Then, the calcined powders were checked by X-ray diffraction method technique to find the appropriate temperature. Finally, the starting composition which was subsequently changed by addition of $Bi_2O_3$, $Na_2CO_3$ or $ZrO_2$ powder at 5, 10 and 15 wt% was prepared by above process and then it was calcined at the appropriate temperature. The calcined powders were investigated once more by using X-ray diffractometer.

### 3. Results and discussion

After as-mixed $Bi_{0.5}Na_{0.5}ZrO_3$ (BNZ) powder was calcined at different temperatures, phase formation was investigated by XRD as shown in Fig. 1. From the results, it was found that the temperatures in range of 700 °C - 750 °C were not enough for completing the reaction. X-ray diffraction analysis showed that the sample contained a large amount of second phases. On the other hand, BNZ powders calcined at 850 °C indicated that the materials began to partially react with alumina crucible and produced less pure BNZ powder. Therefore, based on this study, optimized calcination temperature was found to be 800 °C. Figure 2 showed that the second phases appeared in range of 2θ = 25 – 30, 33, 46 and 50° which were most likely to be the phases of $Bi_2O_3$ and $ZrO_2$. It was expected therefore that addition of $Na_2CO_3$ should help complete the reaction. Hence, addition of 5, 10, 15 wt% $Na_2CO_3$ was carried out and the results are shown in X-ray patterns in Fig. 3. The amount of second phases by a decrease in peak intensity in the region of 2θ from 25-30° was clearly observed. Although both $Na_2CO_3$ and $Bi_2O_3$ have low melting point i.e. 850 and 820 °C, respectively, the volatilization of $Na_2CO_3$ is not as well known as $Bi_2O_3$. In this study, it showed that $Na_2CO_3$ might be more volatile than $Bi_2O_3$ and/or had dissociation problem at calcination temperature used. In order to check this hypothesis, $Bi_2O_3$ and $ZrO_2$ were also separately added into starting mixture. Figure 4 and 5 showed X-ray diffraction results of adding these two compounds, respectively. It showed that both $Bi_2O_3$ and $ZrO_2$ had nearly no effect on phase formation of $Bi_{0.5}Na_{0.5}ZrO_3$. This seemed to be in agreement with the existing second phases observed in Fig. 2. Hence, based on this study, the calcination temperature of 800 °C and addition of excess $Na_2CO_3$ both affected phase purity of synthesized compound. Further improvement of phase purity by re-calcination and changing calcination time will be carried out and reported in the near future.

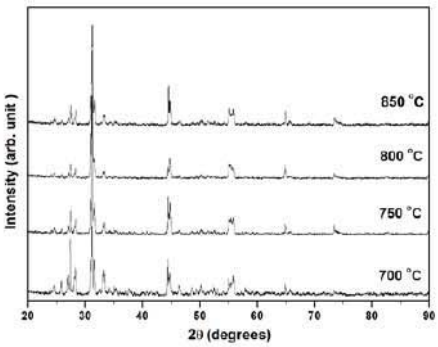


Figure 1. XRD patterns of BNZ powders calcined at different temperature for 2 h.

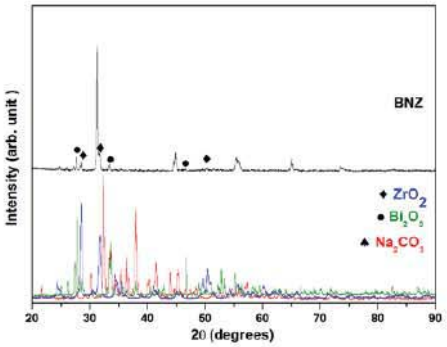


Figure 2. XRD pattern of BNZ powder calcined at 800 °C for 2 h compared with starting powder XRD pattern.

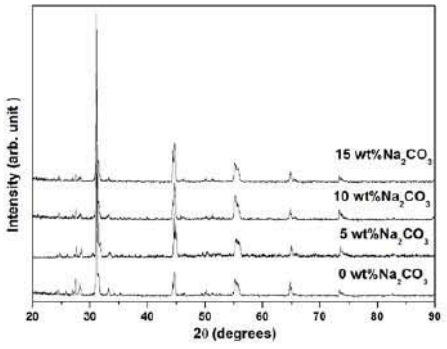


Figure 3. XRD patterns of BNZ/$Na_2CO_3$ powders calcined at 800 °C for 2 h.

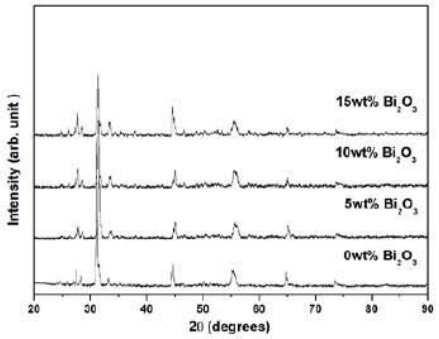


Figure 4. XRD patterns of BNZ/$Bi_2O_3$ powders calcined at 800 °C for 2 h.

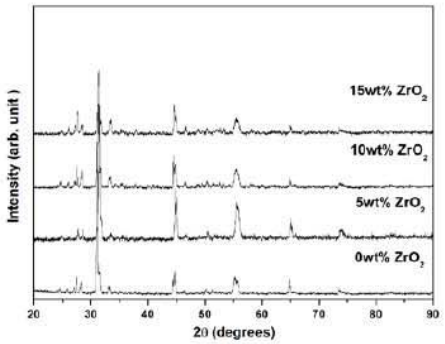


Figure 5. XRD patterns of BNZ/$ZrO_2$ powders calcined at 800 °C for 2 h.

## 4. Conclusion

This research studied several factors affecting phase formation of new lead-free $Bi_{0.5}Na_{0.5}ZrO_3$ compound. Optimized conditions included calcination temperature of 800 °C for 2 h with addition of excess $Na_2CO_3$.

## 5. Acknowledgment

This work is supported by the Thailand Research Fund (TRF), the Commission on Higher Education (CHE). We would also like to acknowledge financial support from the TRF through the Royal Golden Jubilee Ph.D. (RGJ) program.

## References

1. Li, Y., Chen, W., Xu, Q., Zhou, J., Gu, X. and Fang, S., "Electromechanical and dielectric properties of $Na_{0.5}Bi_{0.5}TiO_3$ - $K_{0.5}Bi_{0.5}TiO_3$ - $BaTiO_3$ lead-free ceramics", *Materials Chemistry and Physics,* 94: 328-332 (2005).
2. Nagata, H., Yoshida, M. and Makjuchi, Y., "Large piezoelectric constant and high curie temperature of lead-free piezoelectric ceramic ternary system based on bismuth sodium titanate-bismuth potassium titanate-barium titanate near the morphotropic phase boundary", *Japan Journal of Applied Physics,* 42: 7401 (2003).
3. Smolenskii, G. A., Isupov, V. A., Agranovskaya, A. I. and Krainik, N. N., "New ferroelectric of complex composition", *Soviet Physics and Solid State*, 2[11]: 2651–2654 (1961).
4. Pronin, I. P., Syrnikov, P. P., Isupov, V. A., Egorov, V. M., Zaitseva, N. V. and Ioggr, A. F., "Peculiarities of phase tranditeons in sodium-bismuth titanate", *Ferroelectrics*, 25: 395-397 (1980).
5. Hagiyev, M. S., Ismaizade, I. H. and Abiyev, A. K., "Pyroelectric properties of $Na_{0.5}Bi_{0.5}TiO_3$ ceramics", *Ferroelectrics*, 56: 215-217 (1984).
6. Isupov, V. A., Pronin, T. P. and Kruzina, T. V., "Temperature dependence of birefringence and opalescence of the sodium-bismuth titanate crystals", *Ferroelectrics. Letter*, 2: 205-208 (1984).
7. Yuan, Y., Zhang, S. and Zhou, X., "Effect of La occupation site on the dielectric and piezoelectric properties of $[Bi_{0.5}(Na_{0.5}K_{0.5}Li_{0.1})_{0.5}]TiO_3$ ceramics", *Journal of Materials Science*, 20: 1090-1094 (2009).
8. Watcharapasorn, A., Jiansirisomboon, S. and Tunkasiri, T., "Microstructure and mechanical properties of zirconium-doped bismuth sodium titanate ceramics", *Chiangmai Journal of Science*, 33: 169 (2006).

# Abstracts

## THE 36th CONGRESS on SCIENCE and TECHNOLOGY of THAILAND (STT 36)

## การประชุมวิชาการวิทยาศาสตร์และเทคโนโลยีแห่งประเทศไทย ครั้งที่ 36 (วทท 36)

***Towards a Better Society through Science and Technology***

*วิทยาศาสตร์และเทคโนโลยีเพื่อสังคมที่ดีขึ้น*

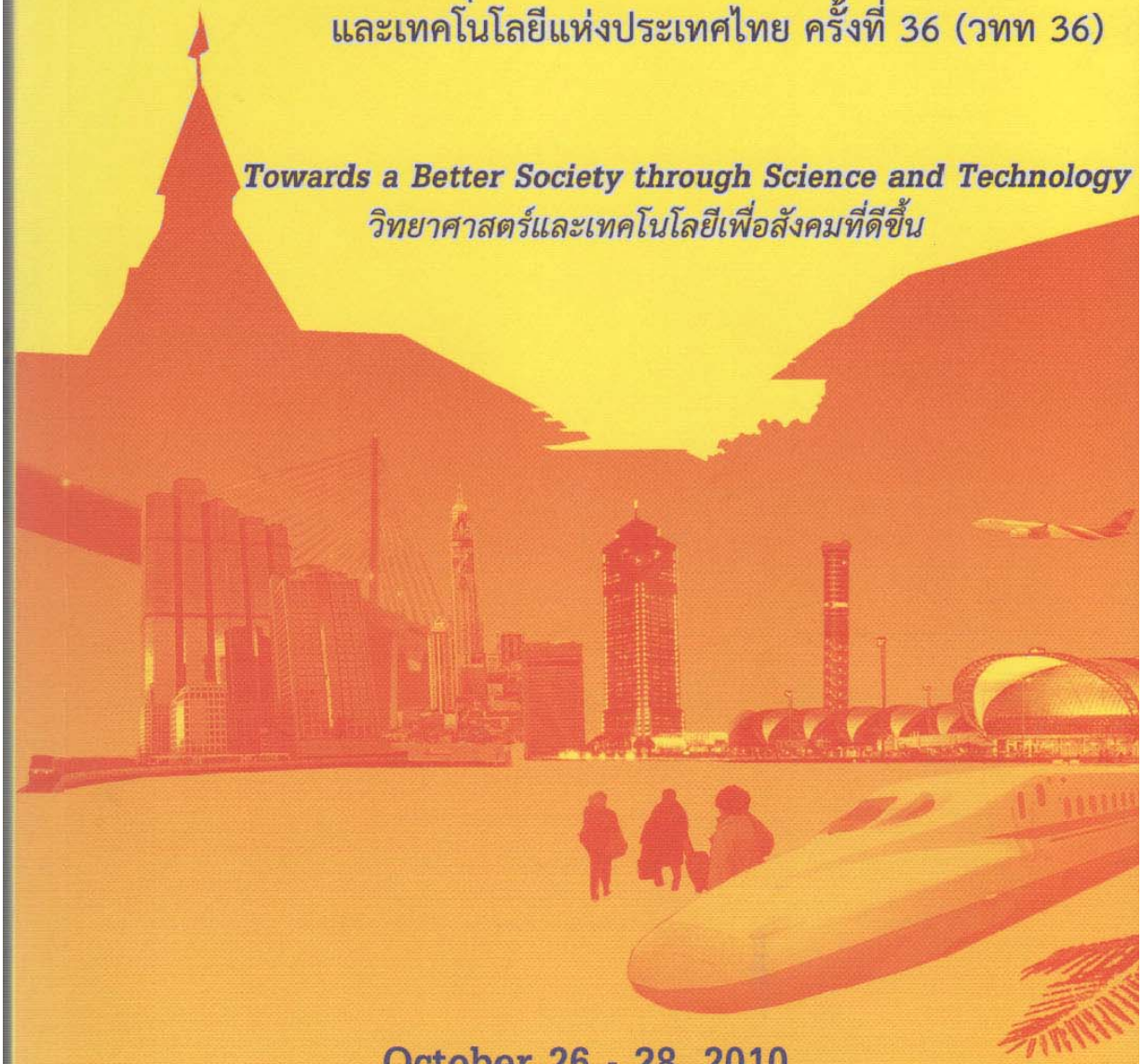

**October 26 - 28, 2010**

Venue: Bangkok International Trade & Exhibition Centre (BITEC). Bangkok, Thailand.

26 - 28 ตุลาคม 2553 ณ ศูนย์นิทรรศการและการประชุมไบเทค กรุงเทพฯ

www.stt36.scisoc.or.th

**Abstract:** In this work, effect of sintering temperature and $W^{6+}$ doping content on phase, densification and microstructure of $Bi_{3.25}La_{0.75}(Ti_{1-x}W_x)_3O_{12}$ or BLTW ceramics when $x$ = 0, 0.01, 0.03, 0.05 0.07, 0.09 and 0.10, was investigated. The BLTW ceramics were sintered at 1000-1150°C for 4 h. The result of phase analysis by X-ray diffraction indicated the existence of orthorhombic phase for all sintering temperatures. At low $WO_3$ doping content (≤ 0.01 mol) showed small increase of particular set of plane {001}. Microstructure of BLTW ceramics showed plate-like grains with random orientation. Increase in $WO_3$ doping concentration reduced both grain size and degree of preferred orientation of the grains. Increasing the $WO_3$ content decreased densification of the ceramics. The microstructural result was well corresponded to the X-ray diffraction result.

**E_E0038: Effects of calcination temperature and excess $Na_2CO_3$ on phase characteristics of bismuth sodium zirconate powder**

Panupong Jaiban, Ampika Rachakom, Sukanda Jainsirisomboon, Anucha Watcharapasorn*
Department of Physics and Materials Science, Faculty of Science, Chiang Mai University, Chiang Mai 50200, Thailand
*e-mail: anucha@stanfordalumni.org

**Abstract:** This research studied the effects of calcination temperature and excess $Na_2CO_3$ on phase characteristics of bismuth sodium zirconate powder. $Bi_{0.5}Na_{0.5}ZrO_3$ powder was prepared by mixed oxide method. The calcination temperature used was in a range of 700 – 850°C. After that, the starting compositions were changed by adding $Na_2CO_3$ in the amount of 0, 5, 10, 15, 20, 25 and 30 wt%. Phase characteristics of powders were analyzed using X-ray diffraction technique. The second phases appearing in BNZ powder were $Bi_2O_3$ and $ZrO_2$ starting powders. These phases were decreased with increasing $Na_2CO_3$ addition.

**E_E0039: Effects of $Nb_2O_5$ on microstructure, phase, and densification of bismuth sodium titanate ceramics**

Napatporn Petnoi, Sukanda Jiansirisomboon, Anucha Watcharapasorn*
Department of Physics and Materials Science, Faculty of Science, Chiang Mai University, Chiang Mai, 50200, Thailand
*e-mail: anucha@stanfordalumni.org

**Abstract:** In this research, the effects of $Nb_2O_5$ (0, 1, 5, 10, 15 and 20 mol%) on microstructure, phase, and densification of bimuth sodium titanate [$(Bi_{0.5}Na_{0.5})TiO_3$ or BNT] ceramics were studied. The powder for making BNT ceramics was prepared by a conventional solid state reaction method. Using calcinations temperature of 800 °C for 2 h. After uniaxial pressing of the powder into discs, green samples were sintered at 1050 °C for 2 h. The results showed that the solubility limit of $Nb_2O_5$ in the BNT system could be as high as 20 mol%. The density of the ceramics tended to increase with $Nb_2O_5$ addition up to 5 mol% and then, density of the ceramics was slightly reduced. The grain size showed a decreasing trend with increasing $Nb_2O_5$ concentration. These results indicated that suitable amount of $Nb_2O_5$ addition could help improve densification and reduce grain growth in BNT ceramics.

**E_E0040: Effect of calcination time on phase formation of $Bi_{0.5}Na_{0.5}Ti_{1-x}Zr_xO_3$**

Ampika Rachakom, Panupong Jaiban, Sukanda Jiansirisomboon, Anucha Watcharapasorn*
Department of Physics and Materials science, Faculty of Science, Chiang Mai University, Chiang Mai 50200, Thailand
*e-mail: anucha@stanfordalumni.org

**Abstract:** The $Bi_{0.5}Na_{0.5}Ti_{1-x}Zr_xO_3$ solid solutions when x= 0.20, 0.35, 0.40, 0.45, 0.60 and 0.80 mole fraction were prepared using a conventional mixed-oxide method. The raw materials were mixed in ethanol using zirconia ball media for 24 h. The calcination temperature was at 700 °C and 2 h dwell time. Phase formation of the powders was examined by X-ray diffraction. The XRD patterns demonstrated nearly all samples possessed rhombohedral structure with increasing Zr concentration, all peaks systematically shifted to the left indicated that the unit cell expanded in agreement with larger $Zr^{4+}$ ions were substituting smaller $Ti^{4+}$ ions. At Zr additives up to 0.60 and 0.80 mole fraction secondary phases appeared which could possibly be Zr-rich phase. Thus, the experimental procedure to decrease the amount of secondary phase using increasing dwell time of calcination from 2 h to 4 h. The results showed those secondary phases were slightly reduced. In addition, it was hypothesized that besides varying dwell time, changing temperature and heating/ cooling rate of calcination should further increase phase purity of BNTZ powder.

# Abstracts

## THE 35th CONGRESS on SCIENCE and TECHNOLOGY of THAILAND (STT 35)

## การประชุมวิชาการวิทยาศาสตร์และเทคโนโลยีแห่งประเทศไทย ครั้งที่ 35 (วทท 35)

### วิทยาศาสตร์และเทคโนโลยีเพื่ออนาคตที่ดีขึ้น

### SCIENCE AND TECHNOLOGY FOR A BETTER FUTURE

*To Celebrate the 35th Anniversary of Faculty of Science, Burapha University*
*To Celebrate the 30th Anniversary of Ministry of Science and Technology*

October 15 - 17, 2009

Venue : The Tide Resort (Bangsaen Beach), Chonburi, Thailand.

15-17 ตุลาคม 2552 ณ เดอะ ไทด์ รีสอร์ท (หาดบางแสน) จังหวัดชลบุรี

WWW.STT35.SCISOC.OR.TH

nanofiber. If these patterns were used as a scaffold, it mimicked the fibrillar structure of collagen in natural having nonwoven and aligned fiber, on extracellular matrix. Extracellular matrix (ECM) is a structural surrounding and supporting cells which composed of ground substance or proteoglycan and collagen fiber which embedded as a 3D network in proteoglycan.

**E_E0005 PROTEIN ANALYSIS BY MALDI-TOF MS USING PLA NANOFIBER MAT SUPPORTS FOR PROTEIN ABSORPTION.**

Noppavan Chanunpanich[1,2], Watana Pinsem[1,2], Boonmee Boonyaphalanant[1], Chonlada Suwanboon[3], Samlee Mankhetkorn[4], Djohan[5], Honsik Byun[6], Jun seo Park[7]
[1]Integrated Nano Science Research Center, Science and Technology Research Institute,
[2]Industrial Chemistry, Faculty of Applied Science, King Mongkut's University of Technology North Bangkok, Thailand
[3]Chemistry, Faculty of Science and Technology, Suan Dusit Rajabhat University, Thailand
[4] Radiologic Technology, Associated Medical Sciences, Chiangmai University, Thailand
[5] Shimazu (Asia Pacific) Pte Ltd, Singapore,
[6]Chemical System Engineering, Keimyung University, Daegu
[7] Chemical Engineering, Hankyong National University, Anseong, Korea Email : ncn@kmutnb.ac.th

**Abstract:** Various PLA nanofiber patterns were successfully fabricated. This paper showed 3 patterns having different on aligned fiber mats. L3, L4 and L6 exhibited %alignment of 39, 66 and 35, respectively. When these nanofiber mat patterns were used for support standard Pepmix-1, having 5 proteins; angiotensin II, angiotensin I, neurotensin, ACTH[1-17], ACTH[18-39], for MALDI-TOF MS investigation, it was found that the L4 pattern exhibited the highest intensity peaks of protein and the less S/N ratio. This is because L4 contained high aligned fiber, resulting large surface area, and enhancing protein adsorption.

**E_E0006 EFFECT OF EXCESS Pb CONTENT AND ANNEALING TEMPERATURE ON PHASE EVOLUTION IN THIN FILMS PZT**

Tharathip Sreesattabud, Manoch Naksata, Anucha Watcharapasorn and Sukanda Jiansirisomboon
Department of Physics and Materials Science, Faculty of Science, Chiang Mai University, Chiang Mai 50200 Thailand. E-mail: sukanda@chiangmai.ac.th

**Abstract:** This research studies effect of annealing temperature and excess Pb addition on phase of thin films lead zirconate titanate (PZT). Sol PZT was synthesized using a modified triol sol-gel processing method. PZT films were prepared by spin coating on (111) platinized silicon substrate. Phase of PZT thin films were investigated using X-ray diffraction technique. The experimental results showed that annealing temperature and excess Pb content were found to affect on phase and orientation of PZT thin films. The results indicated that (111) PZT orientation started to present after being annealed at 400°C and its intensity reduced with increasing annealing temperature. On the other hand, at annealing temperature ≥ 500°C, (100) and (110) orientations tended to increase with increasing annealing temperature. However, pyrochlore phase still appeared even though at annealing temperature 650°C. Increase in excess Pb addition was found to increase crystalline phase, with affected the stability of perovskite crystallization in PZT thin films.

**E_E0007 GRAIN GROWTH AND CRYSTALLOGRAPHIC ORIENTATION OF $Mo^{6+}$-DOPED BLT CERAMICS**

Pasinee Siriprapa, Anucha Watcharapasorn and Sukanda Jiansirisomboon
Department of Physics and Materials Science, Faculty of Science, Chiang Mai University, Chiang Mai 50200, Thailand. E-mail: sukanda@chiangmai.ac.th

Abstract: In this work, effect of $Mo^{6+}$ doping concentration on morphology, growth and crystalline orientation on bismuth lanthanum titanate grain, i.e. $Bi_{3.25}La_{0.75}(Ti_{1-x}Mo_x)_3O_{12}$ (BLTM); when $x$ = 0, 0.01, 0.03, 0.05 0.07, 0.09 and 0.1 mol, respectively. The BLTM powder were prepared by mixed-oxide method and calcined at 750 °C for 4 h dwell time before being pressed and sintered at 1000-1150°C for 4 h. The result showed that BLTM ceramics composed of plate-like grains. Increase in $Mo^{6+}$ doping concentration increased both grain size and degree of preferred orientation of the grains. The result of microstructural investigation was found to be well agreed with observed X-ray diffraction patterns.

**E_E0008 PHYSICAL AND DIELECTRIC PROPERTIES OF LEAD-FREE BISMUTH SODIUM TITANATE ZIRCONATE CERAMICS**

Ampika Rachakom, Sukanda Jiansirisomboon and Anucha Watcharapasorn
Department of Physics and Materials Science, Faculty of Science, Chiang Mai University, Chiang Mai 50200, Thailand. E-mail: anucha@stanfordalumni.org

**Abstract:** This research studied phase formation, microstructure and dielectric properties of lead-free bismuth sodium titanate zirconate ($Bi_{0.5}Na_{0.5}Ti_{1-x}Zr_xO_3$, BNTZ) ceramics when $x$ = 0.20, 0.35, 0.40, 0.45, 0.60 and 0.80 mole fraction, respectively. BNTZ powders were prepared by the conventional mixed oxide method. The synthesized powders were pressed and sintered at 900 ºC for 2 h. The experimental results suggested that BNTZ ceramics still possessed rhombohedral phase with the relative density of 95 % of theoretical value. The grain size seemed to increase with Zr content. In terms of dielectric properties, it was found that addition of Zr caused a decreasing trend in dielectric constant. It was postulated that the expansion of unit cell was the main cause in changing the electrical properties.

**E_E0009 EFFECT OF BNT ADDITION ON PHYSICAL AND DIELECTRIC PROPERTIES OF PZT CERAMICS**

Pharatree Jaita, Anucha Watcharapasorn and Sukanda Jiansirisomboon
Department of Physics and Material Science, Faculty of Science, Chiang Mai University, Chiang Mai 50200, Thailand. E-mail: sukanda@chiangmai.ac.th

**Abstract:** This research studied effect of bismuth sodium titanate (BNT) addition on physical and dielectric properties of lead zirconate titanate (PZT) ceramics. The BNT additional content used in this study were 0, 0.1, 0.5, 1.0 and 3.0 wt%. The ceramics were sintered at 1050-1200 °C in atmosphere. Density, microstructure and phase identifications were carried out using Archimedes' method, scanning electron microscopy and X-ray diffraction technique, respectively. Electrical properties such as dielectric constant and dielectric loss at room temperature were also measured. The results showed that density and grain size of the ceramics tended to decrease with increasing content of BNT addition. Dielectric constant and dielectric loss of the ceramics, however, were found to increase with increasing of BNT content.

**E_E0010 EFFECT OF CuO NANO-PARTICULATES ADDITION ON PHASE AND MICROSTRUCTURE OF PZT CERAMICS**

Methee Promsawat, Anucha Watcharapasorn and Sukanda Jiansirisomboon
Department of Physics and Materials Science, Faculty of Science, Chiang Mai University, Chiang Mai, 50200, Thailand. E-mail: sukanda@chiangmai.ac.th



**Abstract:** This research studies effect of CuO nano-particulates addition on phase and microstructure of PZT ceramics. Firstly, PZT/$x$CuO powders were prepared using a mixed oxide method, when $x$ = 0, 0.1, 0.5 and 1 wt%. The powders were then pressed and sintered at 1250 °C for 2 h. PZT/$x$CuO were investigated in term of phase, density and microstructure using X-ray diffraction technique, Archimedes's method and scanning electron microscope, respectively. The results showed that tetragonality and density of PZT ceramics increased with 0.1 wt% CuO addition. Both parameters, however, tended to decrease with further increase in CuO content. Average grain size was found to sharply decrease with only 0.1 wt% CuO addition.

**E_E0011 EFFECT OF $Si_3N_4$ NANO-PARTICLES ON PHASE AND MICROSTRUCTURE OF $BaTiO_3$ CERAMICS**

Orapim Namsar, Anucha Watcharapasorn and Sukanda Jiansirisomboon
Department of Physics and Materials Science, Faculty of Science, Chiang Mai University, Chiang Mai, 50200, Thailand. E-mail: sukanda@chiangmai.ac.th

**Abstract:** This research studies effect of $Si_3N_4$ nano-particle on phase and microstructure of $BaTiO_3$ ceramics. $BaTiO_3/xSi_3N_4$ powders; $x$ = 0, 0.1, 0.5, 1 and 3 wt% were prepared, pressed and sintered at temperature 1400 °C for 2 h. The $BaTiO_3/xSi_3N_4$ ceramics were investigated in terms of phase, density and microstructure using X-ray diffraction technique, Archimedes's method and scanning electron microscope, respectively. The experimental results indicated crystal structure changes, i.e. tetragonality tended to increase, while relative density of the ceramics with 0.1 wt% $Si_3N_4$ addition was maximum. However, the relative density tended to reduce with increasing content of $Si_3N_4$ > 0.1wt%. Average grain size was found to increase with increasing content of added $Si_3N_4$ nano-particles.

**E_E0012 FABRICATION, ELECTRICAL AND MECHANICAL PROPERTIES OF PZT/PVDF 0-3 COMPOITES**

Pailyn Thongsanitgarn, Anucha Watcharapasorn and Sukanda Jiansirisomboon
Department of Physics and Materials Science, Faculty of Science, Chiang Mai University, Chiang Mai, 50200, Thailand. E-mail: sukanda@chiangmai.ac.th

**Abstract:** This research studied fabrication and properties of $x$PZT/(1-$x$)PVDF composites with 0-3 connectivity, where $x$ = 0, 0.05, 0.1, 0.2, 0.3, 0.4 and 0.5 volume fraction. The experimental results indicated that densities of the composites tended to increase with increasing PZT ceramic content. Investigation on phase and microstructure of the composites revealed well dispersion of PZT in PVDF phase. Dielectric measurement of the composites showed that the dielectric constant increased with increasing of PZT phase while dielectric loss tangent value reduced. The maximum value of dielectric constant was found in 0.5PZT/0.5PVDF composite ($\varepsilon_r \approx 96$). The results of mechanical measurements in terms of hardness, Young's modulus and fracture toughness were found to be improved with increase in PZT content.

## E_E0013 STUDY ON MELT SPINNING OF POLY (METHYL METHACRYLATE) FIBER FOR OPTIC APPLICATIONS

Nanjaporn Sumransin[1*], Chureerat Prahsarn[1], Sirada Phadee[2], Lalita Chompang[2]
[1]National Metal and Materials Technology Center, 114 Paholyothin Rd., Klong Luang, Pathumthani 12120, Thailand *e-mail: nanjaprs@mtec.or.th
[2]Department of Textile Engineering, Rajamangala University of Technology Thanyaburi, Pathumthani 12110, Thailand

**Abstract:** Melt spinning of poly(methyl methacrylate) fibers was studied for its potential use in optics. PMMA fibers were made, using single screw extruder, under different spinning conditions: extruding temperatures, throughputs rates, and draw ratios to investigate their effects on fiber spinnability and optical properties. Experimental results showed that best spinnability was obtained at extruding temperature 270°C and throughput rate 8 rpm such that fibers could be spun continuously without breakage. Poor fiber spinning was obtained at low extruding temperature (230°C) as fiber breakage occurred quite often. This is thought to be due to higher stress acting on fibers when low temperature was employed. PMMA fibers obtained showed good light transmission, thus, have potential for applications on optics in new areas, including decoration and clothing.

## E_E0014 FABRICATION OF LEAD-FREE BISMUTH SODIUM ZIRCONATE CERAMICS

Panupong Jaiban, Sukanda Jiansirisomboon and Anucha Watcharapasorn
Department of Physics and Materials Science, Faculty of Science, Chiang Mai University, Chiang Mai, 50200, Thailand. E-mail: anucha@stanfordalumni.org

**Abstract:** This research studied fabrication of lead-free bismuth sodium zirconate ceramics with formula $Bi_{0.5}Na_{0.5}ZrO_3$. The $Bi_{0.5}Na_{0.5}ZrO_3$ ceramic powder was prepared using a mixed-oxide method and checked for phase purity by X-ray diffraction technique. The powder was pressed into small pellets and sintered at various temperatures ranging from 850-1100 °C. After checking phase purity of ceramics by X-ray diffraction technique and measuring density of the sintered samples, their microstructure was investigated using scanning electron microscopy. Roles of variables such as temperature and time in sintering process were discussed in order to find an optimum condition for fabrication of high-quality bismuth sodium zirconate ceramic.

## E_E0015 MICROSTRUCTURE AND TARNISHING RESISTANCE OF SILVER-COPPER-PALLADIUM JEWELRY STERLING

Kanchana Rithidate, Jirawan Mala and Chutimun Chanmuang*
Faculty of Gems, Burapha University, Chantaburi Campus, Chantaburi, 22170, Thailand
E-mail: chutimun@buu.ac.th

**Abstract:** The Ag-Cu-Pd jewelry sterling in various compositions was casted at 1025°C with the flask temperature by lost-wax technique. Pd950 commercial alloy 0-1.5 wt% was used in order to determine the effect of Pd on silver sterling. The tarnish test was performed by immersing the sample in 0.1% $Na_2S$ and 5% NaCl solutions for 1, 2, 3, 5 and 10 hours. To specify the color space from tarnishing, the surface color difference (DE*) were measured by follow the Commission International d' Eclairage (CIELAB) standard. It was found that the tarnish was improved with high Pd950 content. Microstructural investigation of the as-cast was studied by using an optical microscope (OM) and scanning electron microscope (SEM) equipped with an energy dispersive spectroscopy (EDS). Dendritic phase formations were existed in all the cast structure. Secondary arms width suggested the improvement of dendrite increasing Pd950. The EDS point analysis confirmed the dissolution of Pd not only in silver matrix but also in eutectic phase which present the higher Cu content than that of matrix. However, the mechanical test by Vicker microhardness at 300 gf for 15 s shows no significantly difference in hardness for all the samples.